Analytic model of a magnetically insulated transmission line with collisional flow electrons

W. A. Stygar,[1] T. C. Wagoner,[2] H. C. Ives,[3] P. A. Corcoran,[4] M. E. Cuneo,[1] J. W. Douglas,[4] T. L. Gilliland,[2]
M. G. Mazarakis,[1] J. J. Ramirez,[1] J. F. Seamen,[1] D. B. Seidel,[1] and R. B. Spielman[1]

[1]*Sandia National Laboratories, Albuquerque, New Mexico 87185, USA*
[2]*Ktech Corporation, Albuquerque, New Mexico 87123, USA*
[3]*EG&G, Albuquerque, New Mexico 87107, USA*
[4]*Titan–Pulse Sciences Division, San Leandro, California 94577, USA*

(Received 10 November 2005; published 13 September 2006)

We have developed a relativistic-fluid model of the flow-electron plasma in a steady-state one-dimensional magnetically insulated transmission line (MITL). The model assumes that the electrons are collisional and, as a result, drift toward the anode. The model predicts that in the limit of fully developed collisional flow, the relation between the voltage V_a, anode current I_a, cathode current I_k, and geometric impedance Z_0 of a 1D planar MITL can be expressed as $V_a = I_a Z_0 h(\chi)$, where $h(\chi) \equiv [(\chi+1)/4(\chi-1)]^{1/2} - \ln[\chi + (\chi^2-1)^{1/2}]/2\chi(\chi-1)$ and $\chi \equiv I_a/I_k$. The relation is valid when $V_a \gtrsim 1$ MV. In the minimally insulated limit, the anode current $I_{a,\min} = 1.78V_a/Z_0$, the electron-flow current $I_{f,\min} = 1.25V_a/Z_0$, and the flow impedance $Z_{f,\min} = 0.588Z_0$. {The electron-flow current $I_f \equiv I_a - I_k$. Following Mendel and Rosenthal [Phys. Plasmas **2**, 1332 (1995)], we define the flow impedance Z_f as $V_a/(I_a^2 - I_k^2)^{1/2}$.} In the well-insulated limit (i.e., when $I_a \gg I_{a,\min}$), the electron-flow current $I_f = 9V_a^2/8I_aZ_0^2$ and the flow impedance $Z_f = 2Z_0/3$. Similar results are obtained for a 1D collisional MITL with coaxial cylindrical electrodes, when the inner conductor is at a negative potential with respect to the outer, and $Z_0 \lesssim 40\ \Omega$. We compare the predictions of the collisional model to those of several MITL models that assume the flow electrons are collisionless. We find that at given values of V_a and Z_0, collisions can significantly increase both $I_{a,\min}$ and $I_{f,\min}$ above the values predicted by the collisionless models, and decrease $Z_{f,\min}$. When $I_a \gg I_{a,\min}$, we find that, at given values of V_a, Z_0, and I_a, collisions can significantly increase I_f and decrease Z_f. Since the steady-state collisional model is valid only when the drift of electrons toward the anode has had sufficient time to establish fully developed collisional flow, and collisionless models assume there is no net electron drift toward the anode, we expect these two types of models to provide theoretical bounds on I_a, I_f, and Z_f.

DOI: 10.1103/PhysRevSTAB.9.090401 PACS numbers: 84.70.+p, 52.25.Xz, 52.30.Cv, 47.65.−d

I. INTRODUCTION

When operated at a sufficiently high voltage, a vacuum transmission line experiences space-charge-limited emission of electrons from the line's cathode electrode [1–3]. When the bound current carried by the line's anode electrode is sufficiently high, the resulting magnetic field in the vacuum gap inhibits most of the electrons from striking the anode [4–39]. Such a self-magnetically insulated transmission line (MITL) is commonly used in pulsed-power accelerators to transmit electromagnetic power and energy to a load [40–47].

When designing a MITL for a pulsed-power accelerator, it is useful to have an analytic model that can make predictions about the MITL's electrical performance. Analytic MITL models developed previously assume that the electrons emitted by the MITL's cathode are *collisionless* [7–32,34–39]. In such a MITL, when a steady state has been achieved, the *net* drift velocity of the electrons is parallel to both the anode and cathode electrodes, and is in the direction of the electromagnetic power flow.

The collisionless assumption is, of course, valid only when the collisions to which the flow electrons are subject can be neglected. This is true, for example, when the collisions experienced by the electrons are dominated by *two-body-particle* collisions, such as collisions between the electrons and residual-gas ions in the MITL's anode-cathode (AK) gap. As discussed in Sec. II A, the frequency of such collisions is, for conditions of interest, sufficiently small that their effects can be neglected. However, as discussed in Sec. II B, a number of observations suggest that instabilities in the MITL's flow-electron plasma can result in electrostatic- and electromagnetic-field fluctuations, and that these can subject the electrons to *effective* collisions [16,21,22,24,28,29,33,48–71]. These observations imply that the frequency of such collisions can be sufficiently high to cause the flow electrons to have a small, but non-negligible, component of their drift velocities directed toward the anode.

To quantify the effects such collisions can have on the electrical performance of a MITL, we develop in this article an analytic fluid model of a one-dimensional MITL with *collisional* flow electrons. In Sec. III A, we develop the model for a steady-state 1D planar MITL. In Sec. III B, we use the model to estimate the time required for collisional electrons to establish a steady-state electron-density profile in a MITL's AK gap. In Sec. III C, we develop a general relation between the voltage, anode

current, cathode current, and geometric impedance of a collisional MITL. An expression for the flow impedance is developed in Sec. III D.

In Sec. IV A, we calculate the *minimum anode current* $I_{a,\min}$ required to establish magnetic insulation. It is usually assumed [42,44] that $I_{a,\min}$ is the anode current of a self-limited MITL; i.e., a MITL insulated only by the current flowing across the AK gap at the leading edge of the MITL's power pulse. We follow this convention herein, and assume that a self-limited MITL operates at $I_{a,\min}$. Several workers have speculated that the self-limited anode current may instead be that which is obtained by a *minimum-energy* calculation [12,20]. We discuss such a calculation in Appendix A. In Sec. IV B, we examine the operation of a steady-state collisional MITL in the well-insulated limit ($I_a \gg I_{a,\min}$).

The results presented in Secs. III and IV are developed for a steady-state 1D MITL with *planar parallel electrodes.* In Appendix B, we present relations between the voltage, anode current, cathode current, and geometric impedance of a steady-state 1D MITL with *coaxial cylindrical electrodes*, assuming that the inner conductor is at a negative potential with respect to the outer.

Collisions are expected to broaden the electron sheath of a MITL, and as a result, increase both the anode and electron-flow currents of a MITL, and decrease the MITL's flow impedance. To estimate the extent to which these quantities can be affected, we review in Sec. V *collisionless* MITL models developed by Creedon [8,9], Mendel, Seidel, and Rosenthal [27], and Miller and Mendel [30]. We also present in Sec. V a collisionless model that assumes only that (i) the flow-electron number density is constant throughout the electron sheath, (ii) the electrons at the sheath edge move at the $\mathbf{E} \times \mathbf{B}$ drift velocity, and (iii) the canonical energy of the electrons at the sheath edge is conserved. The Creedon result presented in Sec. V is valid for both planar and coaxial MITLs; the results presented for the other three collisionless models are valid only in planar geometry. In Sec. VI we compare, for a planar MITL, the predictions of these four collisionless models to those of the collisional model.

In Sec. VII, we compare the collisional and Creedon models to experiment. The results of Secs. II–VII are discussed in Sec. VIII.

The steady-state *collisional* model developed in Sec. III, Sec. IV, and Appendix B effectively assumes that the electron velocity throughout the sheath is, to first order, given by the $\mathbf{E} \times \mathbf{B}$ drift velocity. Hence in this model there is, to first order, no net Lorentz force per unit area (i.e., no net Lorentz pressure) on the electrons. The four steady-state *collisionless* models reviewed in Sec. V also assume there is no net Lorentz pressure on the electron sheath. When planar geometry is assumed, these five models use the same *one-dimensional* MITL geometry and hence, the same pressure-balance equation. In Appendix C, we present a general pressure-balance equation for an arbitrary steady-state *three-dimensional* MITL.

II. TWO-BODY-PARTICLE AND EFFECTIVE COLLISIONS

The flow electrons in a MITL are subject to *two-body particle* collisions, and *effective* collisions due to plasma collective effects. *Particle* collisions include electron-electron collisions between the flow electrons themselves, as well as electron-electron, electron-ion, and electron-neutral collisions between the flow electrons and other particles present in the MITL's AK gap. The other particles in the gap include electrons, ions, and neutrals from the residual gas in the gap due to the necessarily imperfect vacuum, and ions and neutrals that evolve from anode- and cathode-electrode plasmas into the gap during the power pulse. *Effective* collisions occur between the flow electrons and electrostatic- and electromagnetic-field fluctuations [16,21,22,24,28,29,33,48–71].

A. Two-body-particle collisions

For MITLs of interest, two-body-particle collisions are dominated by collisions between the flow electrons and the residual-gas ions present in the gap. The *nonrelativistic* electron-ion collision frequency is given by [72]

$$\nu_{ei} = \frac{n_i Z^2 e^4}{4\pi\varepsilon_0^2 m^2 v^3} \ln\Lambda_1. \tag{1}$$

In this expression n_i is the ion number density, Z is the ionization charge state, e is the absolute value of the electron charge, $\ln \Lambda_1$ is the Coulomb logarithm [72], ε_0 is the permittivity of free space, m is the electron rest mass, and v is the electron speed. (Equations in this article are expressed in SI units throughout.)

To estimate a typical value of ν_{ei}, we consider a MITL with a 2-cm AK gap, a 1 MV/cm electric field, and a 1 T magnetic field. (These are characteristic of the parameters of the Z-accelerator MITLs [45–47].) In such a MITL a typical value of v is $\sim 0.2c$, where c is the speed of light. When $n_i \sim 10^{18}$ m^{-3} and $Z = 1$, Eq. (1) finds that $\nu_{ei} \sim 10^2$ s^{-1}. Hence assuming that the characteristic lifetime of flow electrons in such a MITL is, at most, a few tens of nanoseconds, we find that the effects of *two-body* collisions can be neglected.

B. Effective collisions

1. Scaling of the effective collision frequency

The *effective* collision frequency due to plasma collective effects [16,21,22,24,28,29,33,48–71] may be orders of magnitude greater than the two-body collision frequency estimated above. To calculate the effective collision frequency would require modeling the *nonlinear* evolution of flow-electron-plasma instabilities until they achieve a turbulent steady state [53]. To follow this evolution in a self-

consistent and relativistically correct manner would likely require 3D *particle-in-cell* simulations. Ideally, such *numerical* simulations would model the entire width (or circumference) of a MITL to include the full spectrum of possible fluctuations. Such simulations would also have sufficient spatial and temporal resolution, and a sufficient number of particles, to model correctly interactions between the flow electrons and the fluctuating fields.

In addition, it would be desirable for such simulations to include *nonideal* conditions that are often present in a MITL, and that may affect the effective collision frequency. These conditions include (i) the presence of a nonzero-thickness cathode plasma, which is the source of the flow electrons; (ii) nonuniform emission of electrons and ions from the electrodes; (iii) nonuniform evolution of neutrals from the electrodes; (iv) AK-gap asymmetries; (v) drive-voltage asymmetries; (vi) a voltage prepulse that early in time desorbs neutrals from the electrode surfaces; (vii) electromagnetic radiation from the load and other plasmas in the system; (viii) imperfect current contacts between MITL-electrode components; (ix) particles on the electrode surfaces; etc.

We do not present here the results of such simulations, which would be outside the scope of this article. Instead, we use dimensional analysis [73–76] to make the following general observations.

We observe that the effective collision frequency $\nu_{\rm eff}$ of a steady-state turbulent flow-electron plasma is likely to be determined *primarily* by the following variables (here we consider only the magnitudes of these variables, and ignore their signs): the electric force on the electrons per unit volume neE (where n is the flow-electron number density and E is the magnitude of the electric field), the magnetic force per unit volume $ne\upsilon B$ (where B is the magnitude of the magnetic field), and the electron momentum per unit volume $n\gamma m\upsilon$ (where γ is the usual relativistic factor).

Hence we have 4 variables: $\nu_{\rm eff}$, neE, $ne\upsilon B$, and $n\gamma m\upsilon$. Assuming that $\upsilon \sim E/B$, we are left with 3 independent variables and 2 independent dimensions (time and momentum per unit volume). According to the Buckingham Π theorem [73–76], the 3 independent variables are related to each other by a function of $3-2=1$ (i.e., a single) dimensionless quantity. We can choose this quantity to be $\nu_{\rm eff}/\omega_c$, where $\omega_c \equiv eB/\gamma m$ is the relativistic electron-cyclotron frequency, and we can write this function as follows:

$$f\left(\frac{\nu_{\rm eff}}{\omega_c}\right) = 0. \tag{2}$$

Hence under these idealized conditions,

$$\nu_{\rm eff} \propto \omega_c. \tag{3}$$

As discussed in Sec. III C, Eq. (3) is also obtained in a 1D planar MITL when the effective collision frequency $\nu_{\rm eff}$ is constant throughout the sheath.

For a MITL with a 2-cm AK gap, a 1 MV/cm electric field, and a 1 T magnetic field, $\omega_c \sim 2\times 10^{11}\ {\rm s}^{-1}$. Hence when $2\pi\nu_{\rm eff}$ is within 2 orders of magnitude of ω_c, and when the electron lifetime in the MITL is on the order of tens of nanoseconds, a typical flow electron in such a MITL is subject to a number of collisions during its lifetime.

2. Observations that suggest effective collisions play a non-negligible role in MITL operation

The discussion presented above can only suggest that $\nu_{\rm eff} \propto \omega_c$; it cannot predict the proportionality constant. Since the above discussion cannot predict the *magnitude* of $\nu_{\rm eff}$, it cannot predict the effects such collisions can have on the electrical performance of MITLs of interest. However, we note that even if such collisions affect MITL performance at only the ~10% level, they may need to be considered when designing terawatt- and petawatt-class pulsed-power accelerators, given the substantial investment of resources involved in such machines.

The following observations suggest that collisions can, in fact, have non-negligible effects on the performance of MITLs of interest.

(i) Nonrelativistic calculations performed by Buneman, Levy, and Linson [51] show that an electron beam propagating in crossed electric and magnetic fields is *always* unstable (at small wavelengths) due to an electron-cyclotron resonance when $(\omega_p/\omega_c)^2 \gtrsim 0.2$, where ω_p is the electron plasma frequency. For electron sheaths of interest, $(\omega_p/\omega_c)^2$ is on the order of 1 [22,51,55,56]. {For the special case of a sheath with electrons that move in a laminar fashion, and have zero canonical momentum and energy, $(\omega_p/\omega_c)^2 = 1$ throughout the sheath [22,51,56]. This condition is valid for *nonrelativistic* Brillouin flow [51]; it is also valid for *relativistic* Brillouin flow, as demonstrated by Ott and Lovelace [56] and Swegle and Ott [21,22].} Reference [51] also finds that an electron beam propagating in crossed fields can, under certain conditions, be unstable due to velocity shear, and hence be subject to the diocotron instability.

(ii) Experiments performed by Orzechowski and Bekefi [58] on an electron-beam vacuum diode insulated by an externally applied magnetic field demonstrate that a leakage current exists across the diode's AK gap, even when the magnetic field is significantly in excess of that required for insulation. (Please see, for example, Figs. 3 and 4 of [58].) In Ref. [59], Bekefi and Orzechowski reiterate that "sizable current flows are observed even in forbidden regions of the magnetic field in which the diode is presumably insulated magnetically. This current flow is accompanied by copious microwave radiation."

(iii) Bekefi and Orzechowski [59] also observe that "under no conditions could current flow (across the diode's AK gap) be suppressed completely, however large the magnetic field was made." In addition, these authors ob-

serve that ''failure of complete magnetic insulation is not confined to the above experiment but has been observed in all cross-field diode configurations at all voltages.'' Some of these previous observations are described by Mouthaan and Süsskind in Ref. [52]. In fact, as noted in Ref. [58], leakage current across the AK gap of a magnetically insulated diode was observed in 1925 by Langmuir [48].

(iv) In Refs. [59,61], Bekefi and Orzechowski suggest that the leakage current and microwave radiation observed in their vacuum-diode experiments are caused by the diocotron instability of the diode's electron sheath. References [22,28,51] show that this instability is stabilized when one surface of the sheath is in contact with the cathode; however, Buneman has noted that if the cathode surface is covered with plasma, diocotron modes are again possible [49]. (The cathode electrodes of vacuum diodes of interest are covered with plasma for most of the power pulse; it is this plasma that is the source of the diode's electrons.)

(v) Experiments conducted in 1973 by Bernstein and Smith [6] on one of the 4.6-m-long 14-MV MITLs of the Aurora accelerator demonstrate that the self-limited impedance of these MITLs is $0.74Z_0$ (where Z_0 is the MITL's geometric impedance). This is 13% less than the value $0.85Z_0$ predicted by the standard collisionless MITL model, which is the parapotential model developed by Creedon [8,9]. As discussed in Sec. VII, this discrepancy is consistent with the existence of collisions in the MITL's electron sheath.

(vi) Bergeron and colleagues [13] describe measurements performed on a 10-m-long MITL for which the MITL cathode current is consistently 20%–25% less than that predicted by numerical simulations. Hence, the electron-sheath current is significantly higher than expected. This discrepancy is consistent with the existence of collisions that broaden the sheath, and as a consequence, increase the sheath current. The observations of Ref. [13] are reiterated in a review article by Di Capua [26].

(vii) Measurements by Shope and colleagues [15] on a 1.37-m-long MITL powered by the HERMES-II accelerator show that for peak voltages between 3.5 and 10 MV, the self-limited MITL impedance is $\sim 0.64Z_0$, as indicated by Fig. 4(b) of Ref. [15]. This impedance is 12%–23% less than the values $0.73Z_0$–$0.83Z_0$ predicted over this voltage range by the collisionless parapotential MITL model [8,9].

(viii) Di Capua and Sullivan describe in Ref. [18] measurements performed on a 1-m-long 0.7-MV MITL with a 0.5-cm gap. These show that an electron leakage flux of 12 A/cm^2 exists across the MITL's AK gap, after magnetic insulation is established. This leakage is sufficient to result in a loss of $\sim$18% of the total MITL current over a distance of 1 m. The authors suggest that ''this loss could arise from instabilities in the electron flow.''

(ix) In Ref. [16], Bergeron and Poukey describe several 2D numerical simulations of a MITL. They find that, when a parapotential force-balanced electron sheath is launched at the input to the MITL, the sheath ''does not propagate more than a short distance before being totally disrupted, apparently by beam instability.'' They also present evidence of an electron-diffusion process at work in their simulations, and suggest this process ''may explain the anomalous current leakage observed in some experiments''.

(x) In Fig. 6 of Ref. [20], Wang and Di Capua plot the ratio of the MITL anode current to the cathode current obtained in a variety of experiments and numerical simulations. (We caution that many of the reference numbers given in the caption of this figure are incorrect.) The authors conclude that ''most of the observations show a larger fraction of current flowing in the (electron sheath) than that predicted (by their collisionless MITL model).'' Eight of the ratios plotted in this figure were obtained from 2D numerical simulations performed by Poukey and Bergeron [14]. The simulations were performed assuming a 5-m-long MITL, at peak voltages that range from 1 to 10 MV.

(xi) Fully relativistic calculations by Swegle and Ott [21,22] and Swegle [28] demonstrate that the electron sheath in a MITL can be unstable to both the diocotron and magnetron instabilities. (As discussed above, diocotron modes are possible when the MITL's cathode electrode is covered with plasma [49].) The modes with the greatest growth rates are predicted to have frequencies on the order of ω_c [21,22,28]. These predictions are in reasonable agreement with the microwave measurements performed on a vacuum diode by Orzechowski and Bekefi [58,59,61]. Other calculations that examine the stability of a MITL's electron sheath to various perturbations are presented in Refs. [16,24,29,33,49,51,52,55,56,63,64].

(xii) Instability-induced fluctuations appear to play a significant role in the performance of *ion-beam* diodes insulated by an externally applied magnetic field [33,62,65–70]. According to Sudan [62], an insulated ion-diode experiences ''electron loss to the anode through instabilities generated by the velocity shear and electron density gradient'' of the electron sheath. Maron [65] has observed this loss as electron bursts, which ''are accompanied by sharp bursts in microwave radiation,'' and proposes that these bursts may be ''initiated by processes in the cathode plasma.'' Desjarlais [66,67], Westermann and Schuldt [69], and Pointon and co-workers [70] have developed ion-diode models that include collisional broadening (due to field fluctuations) of the electron sheath; these models are in substantially better agreement with experiment than collisionless models.

The above observations suggest that effective collisions due to field fluctuations in the electron sheath of a MITL may, in fact, produce non-negligible effects on a MITL's electrical performance. Hence it is of interest to develop an analytic estimate of the magnitude of such effects.

III. COLLISIONAL-MITL MODEL

A. Relativistic fluid-Maxwell equations

To estimate the effects that field fluctuations can have on the electrical performance of a MITL, we make the following simplifying assumptions. We assume that (i) the electron sheath of a MITL is unstable; (ii) the sheath instabilities cause the flow-electron plasma to evolve to a turbulent steady state; (iii) the turbulence produces electrostatic- and electromagnetic-field fluctuations that subject the electrons to effective collisions; (iv) the turbulent flow-electron plasma can be adequately modeled as a *fluid*; and (v) the effects of fluctuations can be accounted for in a fluid model by a collision term that is given in terms of an effective collision frequency [53]. We develop such a fluid model below, and use it to provide first-order *analytic* estimates of collisional effects.

We begin with the following relativistic fluid-Maxwell equations:

$$\frac{\partial n}{\partial t} + \nabla \cdot (n\mathbf{v}) = 0, \tag{4}$$

$$nm\left(\frac{\partial(\gamma\mathbf{v})}{\partial t} + (\upsilon \cdot \nabla)\gamma\mathbf{v}\right) + ne(\mathbf{E} + \mathbf{v} \times \mathbf{B}) + kT\nabla n = -nm\gamma\mathbf{v}\nu_{\text{eff}}, \tag{5}$$

$$\gamma = \left[1 - \left(\frac{|\mathbf{v}|}{c}\right)^2\right]^{-1/2}, \tag{6}$$

$$\nabla \cdot \mathbf{E} = -\frac{ne}{\varepsilon_0}, \tag{7}$$

$$\nabla \cdot \mathbf{B} = 0, \tag{8}$$

$$\nabla \times \mathbf{E} = -\frac{\partial \mathbf{B}}{\partial t}, \tag{9}$$

$$\nabla \times \mathbf{B} = -\mu_0 ne\mathbf{v} + \frac{1}{c^2}\frac{\partial \mathbf{E}}{\partial t}. \tag{10}$$

In these expressions n is the electron number density, $\mathbf{v}$ is the electron-fluid velocity, m is the electron rest mass, γ is the usual relativistic factor evaluated at the fluid speed $|\mathbf{v}|$, e is the absolute value of the electron charge, $\mathbf{E}$ is the electric field, $\mathbf{B}$ is the magnetic field, k is the Boltzmann constant, T is the electron temperature, ν_{eff} is the frequency of the effective collisions experienced by the electrons, c is the speed of light, ε_0 is the permittivity of free space, and μ_0 is the permeability of free space.

Equations (4) and (5) are the continuity and momentum equations, respectively. Equation (5) makes the simplifying assumption that the pressure tensor is isotropic. We assume T is defined in such a manner that Eq. (5) is relativistically correct. In addition, we neglect in Eq. (5) the $\nabla(\boldsymbol{\mu} \cdot \mathbf{B})$ force due to the intrinsic magnetic moment $\boldsymbol{\mu}$ of an electron [77]; we also neglect effects due to radiation damping [77]. Equation (6) assumes $kT \ll (\gamma - 1)mc^2$. We do not assume an energy equation; instead we assume in Eq. (5) that the electron plasma is isothermal, i.e., that $\nabla T = 0$. The effective collision frequency ν_{eff} is not calculated, and is instead treated as an adjustable parameter.

Assuming the 1D planar-MITL geometry illustrated in Fig. 1, and that a steady state has been achieved, we can express Eqs. (4), (5), and (7)–(10) as follows:

$$\frac{\partial(n\upsilon_x)}{\partial x} = 0, \tag{11}$$

$$nm\upsilon_x\frac{\partial(\gamma\upsilon_x)}{\partial x} + neE_x - ne\upsilon_z B_y + kT\frac{\partial n}{\partial x} = -nm\gamma\upsilon_x\nu_{\text{eff}}, \tag{12}$$

$$nm\upsilon_x\frac{\partial(\gamma\upsilon_z)}{\partial x} + ne\upsilon_x B_y = -nm\gamma\upsilon_z\nu_{\text{eff}}, \tag{13}$$

$$\frac{\partial E_x}{\partial x} = -\frac{ne}{\varepsilon_0}, \tag{14}$$

$$\frac{\partial B_y}{\partial x} = -\mu_0 ne\upsilon_z. \tag{15}$$

Since we assume a 1D MITL, Eqs. (11)–(15) assume that the quantities υ_y, E_y, E_z, B_x, and B_z, and all derivatives with respect to y and z, equal 0. Hence these equations implicitly assume that the magnetic field due to the cross-field electron flux $n\upsilon_x$ is small, so that $\partial B_y/\partial z \sim 0$.

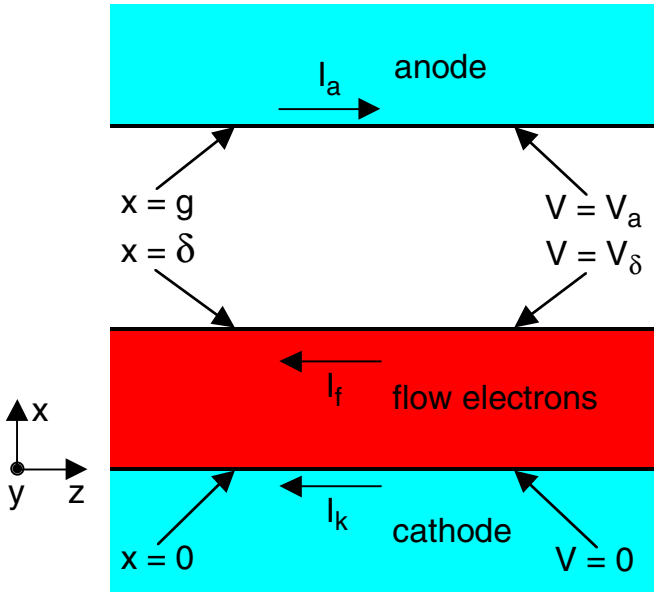

FIG. 1. (Color) Idealized 1D MITL in planar geometry. This figure assumes that the electromagnetic power flows in the positive z direction. The electric and magnetic fields are directed in the negative x and negative y directions, respectively.

From Eq. (13) we obtain

$$v_x = \frac{\alpha v_z}{1 - [\partial(\gamma v_z)/\gamma\omega_c \partial x]}, \tag{16}$$

where

$$\alpha \equiv \frac{\nu_{\text{eff}}}{\omega_c}, \tag{17}$$

$$\omega_c \equiv -\frac{eB_y}{\gamma m}. \tag{18}$$

The quantity ω_c is the relativistic electron-cyclotron (Larmor) frequency. [For the geometry illustrated in Fig. 1, B_y is a negative quantity. The minus sign in Eq. (18) guarantees that ω_c is positive.]

To zeroth order we have that

$$\frac{1}{\omega_c \gamma}\frac{\partial(\gamma v_z)}{\partial x} \sim \frac{v_z}{\omega_c \delta} \sim -\frac{\gamma m v_z}{eB_y \delta}, \tag{19}$$

where δ is the thickness of the electron sheath, as defined in Fig. 1. In the absence of collisions, and when the canonical angular momentum of the electrons is conserved as they move from the cathode into the AK gap, the *collisionless* electron-sheath thickness δ_0 is determined (in part) by the following equation [7–9]:

$$(\gamma m v_z)|_{x=\delta_0} = -e\int_0^{\delta_0} B_y dx. \tag{20}$$

To zeroth order, we can express Eq. (20) as $\gamma m v_z \sim -eB_y\delta_0$. Hence, when collisions are present, and broaden the sheath substantially in excess of the collisionless value (i.e., when $\delta \gg \delta_0$), we have that

$$-\frac{\gamma m v_z}{eB_y \delta} \ll 1. \tag{21}$$

Combining Eqs. (16), (19), and (21) gives

$$v_x = \alpha v_z. \tag{22}$$

Combining Eqs. (12), (17), (18), and (22), we obtain the following expression for the cross-field electron flux:

$$n v_x = \frac{(\alpha n E_x/B_y) + (\alpha kT/eB_y)(\partial n/\partial x)}{1 + \alpha^2\{1 + [\partial(\gamma v_x)/\gamma\nu_{\text{eff}}\partial x]\}}. \tag{23}$$

To zeroth order, we have from Eqs. (17), (18), and (22) that

$$\frac{1}{\gamma\nu_{\text{eff}}}\frac{\partial(\gamma v_x)}{\partial x} \sim \frac{v_x}{\nu_{\text{eff}}\delta} \sim -\frac{\gamma m v_z}{eB_y\delta}. \tag{24}$$

Hence we can use Eqs. (21) and (24) to approximate Eq. (23) as

$$n v_x = \frac{\alpha n E_x}{(1+\alpha^2)B_y} + \frac{\alpha kT}{(1+\alpha^2)eB_y}\frac{\partial n}{\partial x}. \tag{25}$$

Since the electric force on an electron $F = -eE_x$, we can express Eq. (25) as

$$n v_x = n\mu_\perp F - D_\perp \frac{\partial n}{\partial x}, \tag{26}$$

where the cross-field mobility $\mu_\perp$ and diffusion coefficient $D_\perp$ are given by [54,57,78]

$$\mu_\perp \equiv \frac{-\alpha}{(1+\alpha^2)eB_y}, \tag{27}$$

$$D_\perp \equiv \frac{-\alpha kT}{(1+\alpha^2)eB_y}. \tag{28}$$

As expected, the mobility and diffusion coefficient satisfy the Einstein relation [57,78]:

$$D_\perp = \mu_\perp kT. \tag{29}$$

When Eq. (3) is a reasonable approximation, Eq. (17) suggests

$$\alpha \propto \text{const} \tag{30}$$

throughout the electron sheath. Under this condition, Eqs. (28) and (30) give

$$D_\perp \propto \frac{kT}{B_y}, \tag{31}$$

which is identical to the scaling of $D_\perp$ for Bohm (i.e. anomalous) diffusion [50,53,54,57,68,71].

It is clear from Eq. (25) that early in time, before collisions have had a chance to significantly broaden the sheath, the cross-field electron flux (nv_x) at the edge of the sheath is dominated by the diffusion term [the second term on the right-hand side of Eq. (25)]. We expect this to be the case, since at this time, the density gradient $\partial n/\partial x$ is large at the sheath edge. (The density gradient is infinite at the edge of an ideal collisionless sheath.) However, after the gradient has had time to relax, the ratio of the two terms on the right-hand side of Eq. (25) is approximately given by

$$\frac{kT}{neE_x}\frac{\partial n}{\partial x} \sim -\frac{kT}{neE_x}\frac{n}{\delta} \sim \frac{kT}{eV_\delta}. \tag{32}$$

The quantity V_δ is the voltage at the edge of the sheath, as defined by Fig. 1. Assuming

$$kT \ll eV_\delta, \tag{33}$$

we combine Eqs. (25), (32), and (33) to obtain

$$n v_x = \frac{\alpha n E_x}{(1+\alpha^2)B_y}. \tag{34}$$

[When Eq. (33) is not valid, the collisional-MITL model could be developed in terms of a *generalized* electric field [72], defined as $E_{x,\text{gen}} \equiv E_x + (kT/ne)(\partial n/\partial x)$.]

Of course, when collisions are negligible, we can assume $\alpha = 0$. In this limit Eq. (34) predicts $nv_x = 0$ throughout the sheath; i.e., that the cross-field electron flux is negligible. This is, in fact, the assumption made by all steady-state *collisionless* MITL models that assume

laminar flow. (In models that assume *nonlaminar* flow, there is a distribution of electron velocities at each value of x. Such models assume that, at each value of x, the *net* value of $nv_x = 0$.) The *collisional* model we develop in this article assumes α is small but non-negligible; hence we assume

$$0 < \alpha \ll 1. \tag{35}$$

Combining Eqs. (6), (17), (18), (22), (34), and (35) we find that, to first order in α, the electron-fluid momentum equations [Eqs. (12) and (13)] for a collisional MITL can be approximated as follows:

$$v_x = \alpha v_z = -\frac{\nu_{\text{eff}}\gamma m}{eB_y} v_z, \tag{36}$$

$$v_z = \frac{E_x}{B_y}, \tag{37}$$

$$\gamma = \left[1 - \left(\frac{v_z}{c}\right)^2\right]^{-1/2} = \left[1 - \left(\frac{E_x}{cB_y}\right)^2\right]^{-1/2}. \tag{38}$$

Combining Eqs. (11), (36), and (37) we obtain the following expressions for Eq. (11), the electron-fluid continuity equation:

$$\frac{\partial}{\partial x}(nv_x) = \frac{\partial}{\partial x}(\alpha n v_z) = \frac{\partial}{\partial x}\left(\alpha n \frac{E_x}{B_y}\right) = 0. \tag{39}$$

B. Characteristic electron-drift time

Equations (36) and (37) can be used to estimate the time Δt required for flow electrons in a MITL to drift a distance Δx across the MITL's AK gap:

$$\Delta t \sim \frac{(\Delta x)B_y}{\alpha E_x}. \tag{40}$$

When $E_x = -1$ MV/cm, $B_y = -1$ T, and $\alpha = 0.1$, the characteristic time required to drift 2 cm is $\sim$2 ns. Presently, it is not clear what value of α should be used in such a calculation. However, it appears feasible to determine *experimentally* the flux nv_x of electrons that drift across a MITL gap, and from such a measurement [and Eqs. (36) and (37)] obtain, for a given experimental configuration, an estimate of α.

Of course, collisions must play a significant role in any MITL that is sufficiently long, or that has a sufficiently small AK gap, when the characteristic electron lifetime in the MITL is on the order of, or is greater than, the characteristic time required for electrons to drift across a significant fraction of the gap. Alternatively, collisional effects can be neglected in any MITL at sufficiently small values of α.

C. General relation between V_a, I_a, I_k, and Z_0

We expect that the effects of collisions on the electrical performance of a MITL are greatest when the flow-electron sheath has had time to expand across the entire MITL gap; i.e., when a collisional MITL has achieved a steady state. Hence in this section we use the results of Sec. III A to develop a relation between V_a, I_a, I_k, and Z_0 for a steady-state collisional MITL. We define these quantities as follows: V_a is the voltage across the MITL gap, I_a is the magnitude of the bound current flowing in the MITL anode, I_k is the magnitude of the bound current flowing in the MITL cathode, and Z_0 is the geometric vacuum impedance of the MITL; i.e., the transmission line impedance in the absence of flow electrons.

For the 1D planar MITL illustrated in Fig. 1 (which assumes an arbitrary sheath thickness), we have that

$$E_x = -\frac{\partial V}{\partial x}, \tag{41}$$

where $V \equiv V(x)$ is the voltage as a function of x. Hence the voltage at the MITL anode $V_a \equiv V(g)$ can be expressed as [27]:

$$V_a = -E_a g + (E_a \delta + V_\delta), \tag{42}$$

where

$$E_a \equiv E_x(g), \tag{43}$$

$$E_x = -\frac{e}{\varepsilon_0}\int_0^x n dx, \tag{44}$$

$$V_\delta = -\int_0^\delta E_x dx. \tag{45}$$

In these equations E_a is the electric field at the anode (which is identical to the electric field at the edge of the sheath), g is the MITL's AK gap, δ is the thickness of the electron sheath, and V_δ is the voltage at the sheath edge; i.e., $V_\delta \equiv V(\delta)$. (Please see Fig. 1.) Equation (44) assumes $E_k \equiv E_x(0) = 0$; i.e., that the emission of electrons from the cathode is space-charge limited.

Assuming that the width (in the direction perpendicular to the page) of the MITL illustrated in Fig. 1 is w, and that $g/w \ll 1$ (i.e., that transmission-line-edge effects can be neglected), the vacuum impedance Z_0 of a 1D planar transmission line is given by

$$Z_0 = \left(\frac{\mu_0}{\varepsilon_0}\right)^{1/2}\frac{g}{w}. \tag{46}$$

Under these conditions, we find from Ampere's law that the magnitudes of the MITL anode and cathode currents, I_a and I_k respectively, can be expressed as

$$I_a = \left|\frac{B_a w}{\mu_0}\right|, \tag{47}$$

$$I_k = \left| \frac{B_k w}{\mu_0} \right|. \tag{48}$$

The quantities $B_a \equiv B_y(g)$ and $B_k \equiv B_y(0)$ are the magnetic fields at the anode and cathode, respectively.

Equations (41)–(48) are, of course, valid for both collisional and collisionless MITLs [27]. Equations (41)–(48) are used in this section, as well as in Sec. V for the discussion of collisionless MITLs.

Combining Eqs. (14), (15), and (37) we obtain

$$-E_x = \left(\frac{B_y^2 - B_k^2}{\varepsilon_0 \mu_0}\right)^{1/2} = c(B_y^2 - B_k^2)^{1/2}. \tag{49}$$

(For the system outlined in Fig. 1, E_x is a negative quantity.) Equation (49) assumes that $E_k \equiv E_x(0) = 0$. When $x = g$, Eq. (49) becomes

$$-E_a = c(B_a^2 - B_k^2)^{1/2}. \tag{50}$$

Equation (50) is a general relation, approximately valid for the collisional planar MITL considered here, as well as for collisionless MITLs [7,27], and can be obtained for conditions other than those assumed in this section. (Please see, for example, Ref. [7].) In fact, as discussed in Ref. [27], and Appendix C of the present article, Eq. (50) is approximately valid for any steady-state 1D planar MITL whenever $E_k \equiv E_x(0) = 0$, and when all forces per unit area (i.e., all pressures) on the flow electrons other than the Lorentz pressure can be neglected.

Combining Eqs. (18), (38), and (49) we find that for a 1D planar MITL,

$$\omega_c \equiv -\frac{eB_y}{\gamma m} = -\frac{eB_k}{m}; \tag{51}$$

i.e., that ω_c is constant throughout the electron sheath. Hence according to Eqs. (17) and (51), whenever the effective collision frequency ν_{eff} is constant throughout the sheath, so is α. Consequently, Eq. (30) is valid when either the dimensional analysis presented in Sec. II B 1 is valid, or when ν_{eff} is constant throughout the sheath.

Combining Eqs. (42), (46)–(48), and (50), we obtain

$$V_a = Z_0(I_a^2 - I_k^2)^{1/2} + (E_a \delta + V_\delta). \tag{52}$$

{Equation (52) is also obtained in Ref. [27].} The term $(E_a\delta + V_\delta)$ is referred to as the space-charge term [30]. Equation (52) is a general relation, valid for both collisional and collisionless MITLs, whenever Eqs. (42), (46)–(48), and (50) are applicable [27].

To evaluate the right-hand side of Eq. (52) for the collisional MITL modeled in Sec. III A, we consider Eq. (39), which implies

$$\alpha n v_z \propto \alpha n \frac{E_x}{B_y} \propto \text{const.} \tag{53}$$

When $\alpha > 0$, the electron sheath (in the steady state) extends across the entire AK gap of the MITL. In this case the edge of the sheath is at the anode ($\delta = g$), and from Eqs. (42) and (45) we find that Eq. (52) becomes simply

$$V_a = V_\delta = -\int_0^g E_x dx. \tag{54}$$

To determine E_x, we recall that the dimensional arguments presented in Sec. II B 1 suggest α is constant throughout the electron sheath [Eq. (30)]. As discussed above, Eq. (30) is also obtained whenever ν_{eff} is constant. In either case, if we assume Eq. (30), then Eq. (53) suggests nv_z is also constant. Under this condition Eq. (15) finds that B_y is a linear function of x:

$$B_y = Cx + B_k, \tag{55}$$

$$C \equiv \frac{B_a - B_k}{g}. \tag{56}$$

Combining Eqs. (49) and (56) gives

$$E_x = -c(C^2x^2 + 2CxB_k)^{1/2}. \tag{57}$$

Combining Eqs. (46)–(48), (54), (56), and (57) we obtain [79]

$$V_a = I_a Z_0 h(\chi), \tag{58}$$

where

$$h(\chi) \equiv \frac{1}{2}\left[\left(\frac{\chi+1}{\chi-1}\right)^{1/2} - \frac{\ln[\chi + (\chi^2-1)^{1/2}]}{\chi(\chi-1)}\right], \tag{59}$$

$$\chi \equiv \frac{I_a}{I_k}. \tag{60}$$

Equation (58) is a general relation between V_a, I_a, I_k, and Z_0 for a 1D planar collisional MITL in the steady state, assuming α is constant and that $0 < \alpha \ll 1$. It is interesting to note that under these conditions, the relation between V_a, I_a, I_k, and Z_0 is independent of α. Equation (58) can also be expressed in terms of the MITL electron-sheath current, which we refer to as the electron-flow current I_f. As suggested by Fig. 1, I_f is defined as follows:

$$I_f \equiv I_a - I_k. \tag{61}$$

Equation (58) assumes a 1D planar collisional MITL with parallel-plate electrodes. In Appendix B, we extend this model to coaxial cylindrical electrodes, assuming that the inner electrode is at a negative potential with respect to the outer. In this case the general relation between V_a, I_a, I_k, and Z_0 is given as Eq. (B1). We note that Eq. (B1) is not given *explicitly* in terms of Z_0, since Eq. (B1) is more naturally expressed in terms of the MITL AK gap and the radius of the inner MITL conductor.

D. Flow impedance Z_f

References [35–38] define the *electrical flow impedance* Z_f of a MITL by the following expression:

$$V_a = Z_f(I_a^2 - I_k^2)^{1/2}. \tag{62}$$

As discussed in Ref. [36], the *electrical* flow impedance is to be distinguished from the *magnetic* flow impedance. For a 1D planar MITL, the *electrical* flow impedance $Z_f = g'Z_0/g$, where g' is the distance between the MITL anode and the centroid of the MITL's flow-electron *charge* density [36]. Similarly, the *magnetic* flow impedance is proportional to the distance between the anode and the centroid of the MITL's flow-electron *current* density [36]. Following the convention established in Ref. [36], we refer to the electrical flow impedance Z_f, which is defined by Eq. (62), as simply the flow impedance.

Combining Eqs. (58)–(60) and (62), we find that the flow impedance of a collisional planar MITL can be expressed as follows:

$$Z_f = \frac{Z_0}{2}\left[\frac{\chi}{\chi - 1} - \frac{\ln[\chi + (\chi^2 - 1)^{1/2}]}{(\chi^2 - 1)^{1/2}(\chi - 1)}\right]. \tag{63}$$

We can readily verify Eq. (63) in one limit. Equations (37), (47)–(49), and (60) predict that when $\chi \to \infty$, the electron speed $v_z \to c$ throughout the sheath. In this limit Eq. (53) predicts that the electron-charge density n approaches a constant value throughout the sheath. Hence in this case the charge-density centroid approaches a point midway between the anode and cathode; i.e., $g' \to g/2$. This is consistent with Eq. (63), since as $\chi \to \infty$, $Z_f \to Z_0/2$.

Since collisions move the charge-density centroid toward the anode, they decrease Z_f. Hence, when V_a is held fixed, then Eqs. (47), (48), (50), and (62) predict that such motion of the centroid increases E_a, and hence (from Gauss's Law) the total flow-electron charge per unit area in the MITL. Collisional drift of the electrons toward the anode also increases the average value of the electron speed v_z, since whenever Eqs. (37) and (49) are valid, the magnitude of v_z increases as x increases. Consequently, we expect the drift of electrons toward the anode to increase the electron-flow current I_f, in addition to decreasing Z_f.

The arguments above suggest that collisions also move the current-density centroid closer to the anode. Such movement decreases the *effective* impedance of a collisional MITL, as seen by the MITL's driving circuit. Consequently, for a given MITL configuration, at a given value of V_a, we expect collisional broadening to increase the MITL anode current I_a above the value obtained in the absence of collisions.

These predictions are quantified in Sec. VI using the results developed above, in Sec. IV, and in Sec. V.

IV. COLLISIONAL-MITL OPERATION IN THE MINIMALLY INSULATED AND WELL-INSULTED LIMITS

A. Collisional-MITL operation when $I_a = I_{a,\min}$

In this section we present an estimate of the minimum anode current required to establish magnetic insulation in a 1D planar collisional MITL. Strictly speaking, the flow electrons of a collisional MITL are not insulated, since the electrons drift across the magnetic field until they strike the anode. In this case, we define insulation to be achieved when the pressure balance given by Eq. (50) is approximately satisfied, so that Eq. (58) is valid.

The minimum anode current is calculated using Eq. (58). The calculation is performed by finding, for given values of V_a and Z_0, the value of χ that minimizes I_a. This is also the value of χ that maximizes $h(\chi)$. We find numerically from Eq. (58) that the minimum anode current is approximately given by

$$I_{a,\min} = 1.78\frac{V_a}{Z_0}. \tag{64}$$

Since $h(\chi)$ is independent of V_a, the constant on the right-hand side of Eq. (64) is also independent of V_a.

The anode current is a minimum ($I_a = I_{a,\min}$) when

$$\chi_{\min} \equiv \left.\frac{I_a}{I_k}\right|_{\min} = 3.35. \tag{65}$$

(The quantity $\chi_{\min}$ is the value of χ at which $I_a = I_{a,\min}$.) When $I_a = I_{a,\min}$, the flow-electron current I_f is given by

$$I_{f,\min} = 0.701 I_{a,\min} = 1.25\frac{V_a}{Z_0}. \tag{66}$$

According to Eqs. (63) and (65), the flow impedance of a collisional MITL when $I_a = I_{a,\min}$ is approximately

$$Z_{f,\min} = 0.588 Z_0. \tag{67}$$

We note that a flow impedance on the order of $Z_0/2$ is observed in the MITL experiments described by Cuneo and co-workers [43]. However, as demonstrated by Rosenthal [41], this low impedance is caused by electrons emitted from the multiple cathodes of the positive-polarity MITL-voltage adder used in the experiments, and is not due to collisional effects.

B. Collisional-MITL operation when $I_a \gg I_{a,\min}$

When the anode current I_a is significantly in excess of the minimum required to establish magnetic insulation (i.e., when $I_a \gg I_{a,\min}$), it can be shown from Eqs. (58) and (59) that

$$\chi \to 1. \tag{68}$$

In this limit we obtain from Eqs. (62) and (63) the following expression:

$$V_a = \tfrac{2}{3} Z_0 (I_a^2 - I_k^2)^{1/2}. \quad (69)$$

Equation (69) is an approximate relation between V_a, Z_0, I_a, and I_k for a steady-state collisional MITL in the well-insulated limit. When expressed in terms of I_f, V_a, Z_0, and I_a, Eq. (69) can be written as

$$I_f = \frac{9 V_a^2}{8 I_a Z_0^2}. \quad (70)$$

As indicated by Eqs. (62) and (69), in the limit $\chi \to 1$,

$$Z_f = \frac{2 Z_0}{3}. \quad (71)$$

Consequently, according to Eqs. (67) and (71), the flow impedance of a well-insulated collisional MITL (i.e., when $I_a \gg I_{a,\min}$) is ~13% greater than it is when $I_a = I_{a,\min}$.

V. COLLISIONLESS-MITL MODELS

As suggested by Eq. (34), we expect that in the *absence* of collisions (i.e., when $\alpha = 0$ and $\delta = \delta_0$), the flux $n v_x$ of flow electrons equals 0 for all values of x inside the electron sheath:

$$n v_x = 0. \quad (72)$$

In this section, we briefly review three *analytic* steady-state collisionless MITL models that are developed in Refs. [8,9,27,30]. In addition, we describe a fourth model that makes assumptions that differ slightly from those made previously. (We note that the four models predict somewhat different values for the collisionless sheath thickness δ_0.)

The Creedon model, which is reviewed below, assumes laminar flow, and hence Eq. (72). The other three models assume nonlaminar electron flow, and hence implicitly assume that at each point in the sheath there is a distribution of electron velocities. Nevertheless, these models also, in effect, assume Eq. (72), since these models assume that at each point in the sheath, the *net* value of $n v_x = 0$.

The four models are valid in 1D planar geometry. The Creedon model [8,9] is also valid for a MITL with coaxial electrodes in cylindrical geometry, when the inner electrode is at a negative potential with respect to the outer.

A. Creedon

The 1D steady-state MITL model developed by Creedon in Refs. [8,9] is often referred to in the literature as the parapotential MITL model. This model assumes Eqs. (37), (38), and (72)—i.e., that the flow electrons move in a laminar fashion at the $\mathbf{E} \times \mathbf{B}$ drift velocity. References [8,9] also implicitly assume Eqs. (41)–(50) and (52) (when a planar MITL is assumed). In addition, Refs. [8,9] assume that the flow electrons are born at the cathode, and that the canonical momentum and energy of the electrons are constant throughout the sheath; i.e., that for $0 \le x \le \delta_0$,

$$\gamma m v_z = -e \int_0^x B_y(u) du, \quad (73)$$

$$(\gamma - 1) mc^2 = -e \int_0^x E_x(u) du. \quad (74)$$

Under these assumptions Creedon [8,9] finds that

$$V_a = Z_0 (I_a^2 - I_k^2)^{1/2} - \frac{mc^2}{e} \{ (\chi^2 - 1)^{1/2} \times \ln[\chi + (\chi^2 - 1)^{1/2}] + (1 - \chi) \}, \quad (75)$$

where χ is defined by Eq. (60).

As mentioned above, Eq. (75) is also valid for a MITL with coaxial electrodes, when the inner electrode is negative. In this case, the geometric MITL impedance is given by $Z_0 = (\mu_0 / 4\pi^2 \varepsilon_0)^{1/2} \ln(r_a / r_k)$, where r_a and r_k are the radii of the outer and inner electrodes, respectively.

We note that Ron, Mondelli, and Rostoker [7] develop a *semianalytic* 1D collisionless MITL model that does not assume laminar flow. Instead of Eqs. (37) and (38), Ref. [7] assumes that the electrons are born at the cathode, follow cycloidal-like orbits in the sheath, and have constant canonical momentum and energy throughout. (Reference [7] *does* implicitly assume Eq. (72); i.e., that at every x between 0 and δ_0, the *net* value of $n v_x = 0$. However, at each value of x, half the electrons have a positive $n v_x$, and the other half a negative $n v_x$.} Although these electron orbits are considerably different than the laminar orbits assumed by Creedon, the two models give similar expressions for V_a, as discussed in Ref. [9].

B. Mendel, Seidel, and Rosenthal

The 1D steady-state planar-MITL model developed by Mendel, Seidel, and Rosenthal in Ref. [27] is similar to the model developed by Creedon [8,9], since both use Eqs. (41)–(48), (50), (52), and (72). However, Ref. [27] does not assume that the electron flow is laminar; i.e., Ref. [27] does not require Eqs. (37), (38), and (49) to be valid. Instead, Ref. [27] considers more general flows, and obtains an expression for V_a in terms of form factors F and G (defined in [27]). The expression obtained for V_a (in terms of I_a, I_k, and Z_0) is insensitive to the precise value of F, and for many flows of interest, $G \sim 1$ [27]. When $F = G = 1$ (as is assumed in Ref. [30]), the expression for V_a becomes

$$V_a = Z_0 (I_a^2 - I_k^2)^{1/2} - \frac{mc^2}{e} (\chi - 1) \{ [2(\chi + 1)]^{1/2} - 1 \}. \quad (76)$$

C. Miller and Mendel

In Appendix A of Ref. [30], Miller and Mendel develop an expression for V_a that is simpler than either Eq. (75) or

(76). Reference [30] uses nonrelativistic arguments to estimate that, near the cathode, the electron number density n is given by

$$n = \frac{\varepsilon_0 B_k^2}{m}. \tag{77}$$

Reference [30] then makes the *ansatz* that the density is constant throughout the sheath at the value given by Eq. (77). Combining Eq. (41)–(48), (50), (52), (72), and (77) gives

$$V_a = Z_0(I_a^2 - I_k^2)^{1/2} - \frac{mc^2}{2e}(\chi^2 - 1), \tag{78}$$

which is the expression presented in Appendix A of [30].

D. Constant-electron-density model

Although Eq. (78) is considerably simpler than either Eq. (75) or (76), Eq. (78) requires the assumption that the electron density throughout the sheath is given by Eq. (77). We find that an expression similar to Eq. (78) can be obtained without making this assumption.

Following Refs. [30,32], we assume that the electron number density in the sheath is constant. Following [8,9,32], we assume that the electrons at the sheath edge ($x = \delta_0$) move at the $\mathbf{E} \times \mathbf{B}$ drift velocity:

$$v_z(\delta_0) = \frac{E_x(\delta_0)}{B_y(\delta_0)}. \tag{79}$$

Assuming that the canonical energy of the electrons at the sheath edge is the same as at the cathode [27], the relativistic factor γ of the electrons at the edge is given by

$$\gamma(\delta_0) \equiv \left[1 - \left(\frac{v_z(\delta_0)}{c}\right)^2\right]^{-1/2} = 1 + \frac{eV_{\delta_0}}{mc^2}. \tag{80}$$

Combining Eqs. (41)–(48), (50), (52), (72), (79), and (80), we obtain the following relation:

$$V_a = Z_0(I_a^2 - I_k^2)^{1/2} - \frac{mc^2}{e}(\chi - 1). \tag{81}$$

This relation can also be obtained from the model developed in Ref. [27] (and reviewed in Sec. V B) if one assumes that the form factors F and G defined in [27] are given by $F = 1$ and $G = [1 + (eV_{\delta_0}/2mc^2)]^{-1/2}$.

Although Eqs. (78) and (81) are similar, the former is easier to work with analytically, since Eq. (78) can be used to give I_a as a 3rd-order polynomial in χ^2, whereas Eq. (81) gives I_a as a 4th-order polynomial in χ.

Lawconnell and Neri [32] also develop a 1D steady-state MITL model assuming a constant-electron-density profile. (In addition, these authors develop a model that assumes a quadratic density profile [32].) The *semianalytic* models of Ref. [32] assume laminar flow [Eqs. (37) and (72)], and are developed for MITLs with coaxial electrodes.

VI. COMPARISON OF THE COLLISIONAL AND COLLISIONLESS MODELS

A. $I_a = I_{a,\min}$

The 1D planar collisional-MITL model developed in Secs. III and IV predicts that the minimum anode current $I_{a,\min}$ required to satisfy Eq. (58) is given by Eq. (64). To calculate $I_{a,\min}$ for the four collisionless models represented by Eqs. (75), (76), (78), and (81), we express each of these equations in the following form:

$$I_a Z_0 = H(V_a, \chi), \tag{82}$$

where $H(V_a, \chi)$ is a function that differs for each of the four models. For each model, we use Eq. (82) to find numerically the minimum value of the product $I_a Z_0$ as a function of V_a.

In Fig. 2, we plot $I_{a,\min}Z_0/V_a$ as a function of V_a for the collisional model and the four collisionless models, assuming 1D planar-MITL geometry. Figure 2 demonstrates that in spite of the substantially different physical assumptions made by the four collisionless models, all predict a similar dependence of $I_{a,\min}Z_0/V_a$ on V_a. This can be explained as follows [27,30]: The first term on the right-hand side of each of Eqs. (75), (76), (78), and (81) is identical to the first term on the right-hand side of Eq. (52). The second term on the right-hand side of each of Eqs. (75), (76), (78), and (81) is different for each of the four models, since the models

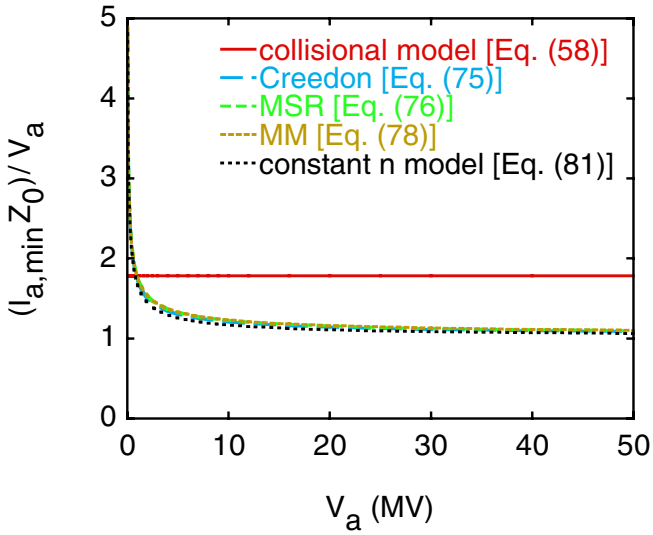

FIG. 2. (Color) The ratio $I_{a,\min}Z_0/V_a$ as a function of V_a for a 1D planar MITL, plotted for 50 kV $\leq V_a \leq$ 50 MV. The quantity $I_{a,\min}$ is the minimum anode current required to establish magnetic insulation. The ratio is plotted for the collisional model [Eq. (58)] and four collisionless models [Eqs. (75), (76), (78), and (81)]. Equation (75) is obtained by Creedon [8,9], Eq. (76) by Mendel, Seidel, and Rosenthal [27], and Eq. (78) by Miller and Mendel [30]. [Eq. (81) is obtained in the present article.] When $V_a \gtrsim 1$ MV, experimentally observed values of $I_{a,\min}$ are expected to fall between the collisional and collisionless limits.

give different expressions for the space-charge term [the second term on the right-hand side of Eq. (52)]. Nevertheless, the four models predict a similar dependence of $I_{a,\min}Z_0/V_a$ on V_a since, as first observed by Refs. [27,30], the space-charge term is, for the collisionless models, typically much less than the first term on the right-hand side of Eq. (52).

As indicated by Fig. 2, when $V_a \gtrsim 1$ MV, the collisional model predicts that more anode current is required to establish magnetic insulation than is required by the four collisionless models.

When $V_a < 1$ MV, the collisional model predicts that less current is required; however, this prediction is not meaningful. We expect that in any MITL, collisional effects can be neglected at the location in the MITL when the flow electrons are first launched, and that a steady-state collisional profile can only develop downstream. Hence before collisional effects become significant, a MITL is *effectively* collisionless, and the current required to establish insulation at that point is that calculated by the collisionless models. Consequently the minimum value of I_a required to establish insulation must always be greater than or equal to that predicted by the collisionless models. Hence as indicated by Fig. 2, when $I_a \sim I_{a,\min}$, Eq. (58) can only be valid when $V_a \gtrsim 1$ MV.

Figure 3 plots the quantity $I_{f,\min}Z_0/V_a$ as a function of V_a for the collisional model and four collisionless models.

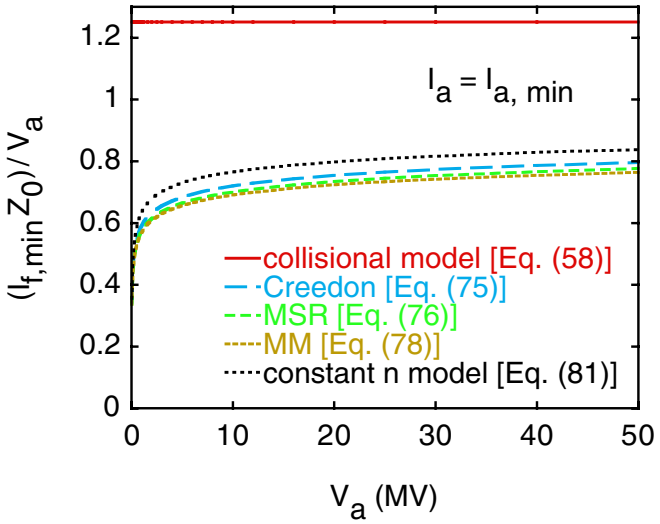

FIG. 3. (Color) The ratio $I_{f,\min}Z_0/V_a$ as a function of V_a for a 1D planar MITL, plotted for 50 kV $\leq V_a \leq$ 50 MV. The quantity $I_{f,\min}$ is the electron-flow current when $I_a = I_{a,\min}$. The ratio is plotted for the collisional model [Eq. (58)] and four collisionless models [Eqs. (75), (76), (78), and (81)]. Equation (75) is obtained by Creedon [8,9], Eq. (76) by Mendel, Seidel, and Rosenthal [27], and Eq. (78) by Miller and Mendel [30]. [Eq. (81) is obtained in the present article.] When $V_a \gtrsim$ 1 MV, experimentally observed values of $I_{f,\min}$ are expected to fall between the collisional and collisionless limits.

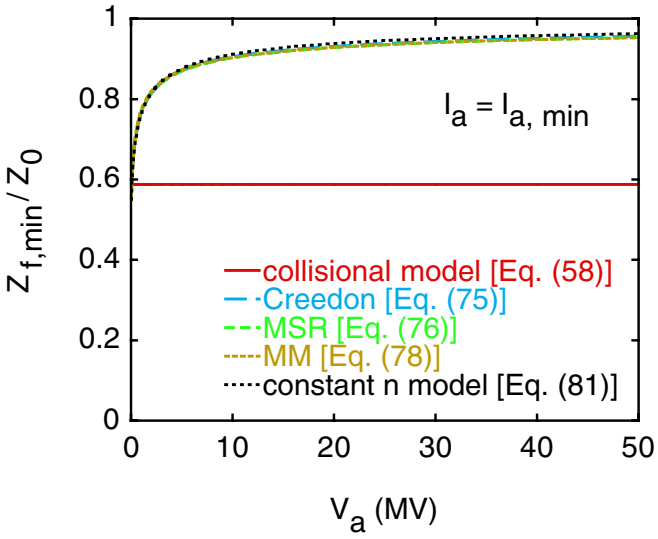

FIG. 4. (Color) The ratio $Z_{f,\min}/Z_0$ as a function of V_a for a 1D planar MITL, plotted for 50 kV $\leq V_a \leq$ 50 MV. The quantity $Z_{f,\min}$ is the flow impedance when $I_a = I_{a,\min}$. The ratio is plotted for the collisional model [Eq. (58)] and four collisionless models [Eqs. (75), (76), (78), and (81)]. Equation (75) is obtained by Creedon [8,9], Eq. (76) by Mendel, Seidel, and Rosenthal [27], and Eq. (78) by Miller and Mendel [30]. [Eq. (81) is obtained in the present article.] When $V_a \gtrsim$ 1 MV, experimentally observed values of $Z_{f,\min}$ are expected to fall between the collisional and collisionless limits.

Figure 4 plots $Z_{f,\min}/Z_0$ as a function of V_a. All five plots in each of Figs. 3 and 4 assume $I_a = I_{a,\min}$, where $I_{a,\min}$ is the minimum anode current required to establish magnetic insulation, as determined by each model.

As indicated by Fig. 3, the normalized flow current $I_{f,\min}Z_0/V_a$ predicted by the collisional model is greater than that predicted by the four collisionless models. As indicated by Fig. 4, the normalized flow impedance $Z_{f,\min}/Z_0$ is less (at high voltages). For the reasons discussed above, Figs. 3 and 4 are meaningful only when $V_a \gtrsim 1$ MV.

B. $I_a \gg I_{a,\min}$

For some applications, routine and reliable MITL operation requires that the MITL be well insulated during most of the power pulse [45–47]. We define a MITL to be well insulated when $I_a \gg I_{a,\min}$. It can be shown that, for the collisional and collisionless models, when $I_a \gg I_{a,\min}$ then $\chi \to 1$; the converse is also true.

Assuming the 1D planar collisional model developed in Secs. III and IV, and that $\chi \to 1$, the electron-flow current I_f and flow impedance Z_f are given by Eqs. (70) and (71), respectively.

For all four of the collisionless models described in Sec. V, we find that when $\chi \to 1$,

$$V_a = Z_0(I_a^2 - I_k^2)^{1/2}. \tag{83}$$

TABLE I. Theoretical expressions for the electron-flow current I_f and flow impedance Z_f of a steady-state 1D planar MITL in the well-insulated limit (i.e., when $I_a \gg I_{a,\min}$). The collisional predictions are given by Eqs. (70) and (71); the collisionless predictions by Eqs. (84) and (85). The collisional predictions are also valid to first order for coaxial MITLs when $Z_0 \lesssim 40\ \Omega$; the collisionless predictions are valid for coaxial MITLs with arbitrary impedance. We expect that experimentally observed values of I_f and Z_f will fall between the idealized collisional and collisionless values.

MITL parameter	Prediction of the collisional model when $I_a \gg I_{a,\min}$	Prediction of the collisionless models when $I_a \gg I_{a,\min}$
I_f	$9V_a^2/8I_aZ_0^2$	$V_a^2/2I_aZ_0^2$
Z_f	$2Z_0/3$	Z_0

Hence, in this limit, the electron-flow current I_f and the flow impedance Z_f can be approximated as

$$I_f = \frac{V_a^2}{2I_aZ_0^2}, \tag{84}$$

$$Z_f = Z_0. \tag{85}$$

According to Eqs. (70) and (84), at given values of V_a, I_a, and Z_0, the electron-flow current I_f of a well-insulated collisional planar MITL is a factor of $9/4$ greater than it is when the MITL is collisionless. According to Eqs. (71) and (85), the flow impedance of a well-insulated collisional MITL is 33% less. These comparisons are summarized in Table I.

We note that Eqs. (70), (71), (84), and (85) are valid for arbitrary values of V_a, Z_0, and I_a, requiring only that $I_a \gg I_{a,\min}$ (i.e., that $\chi \rightarrow 1$).

VII. COMPARISON OF THE COLLISIONAL AND COLLISIONLESS MODELS WITH EXPERIMENT

The collisional model [Eqs. (58) and (B1)] is valid only when the drift of electrons toward the anode has had sufficient time to broaden the electron sheath until a steady-state configuration has been achieved. The collisionless models [Eqs. (75), (76), (78), and (81)] are valid in the opposite limit; i.e., when collisional broadening of the sheath can be neglected. Consequently, we expect that *experimentally observed* electrical parameters of a real MITL will fall *between* the values predicted in these two limits.

A *definitive* comparison of theory with experiment may not be presently possible because of the limited data available in the literature on long MITLs with small AK gaps; i.e., in the parameter regime most likely to be significantly affected by collisions. In addition, as is well known, measurements of MITL voltages and currents at magnitudes of interest are inherently difficult to perform with great accuracy. Nevertheless, in this section we compare available data with predictions. The comparison suggests that collisions can, in fact, have non-negligible ($\gtrsim 10\%$) effects on the electrical performance of physically relevant MITLs.

The data and corresponding predictions are summarized in Table II. Most of the measurements summarized in the table were performed on *self-limited* MITLs. We define a MITL to be self-limited when it is insulated only by the current flowing across the AK gap at the leading edge of the MITL's power pulse. We follow conventional practice [42,44] and *assume* that when a MITL is self-limited, $I_a = I_{a,\min}$; i.e., that the anode current of a self-limited MITL is the *minimum* required to establish magnetic insulation. Hence we also assume that when a MITL is self-limited, $I_f = I_{f,\min}$ and $Z_f = Z_{f,\min}$. Consequently, the comparisons in Table II between the self-limited-MITL results and corresponding predictions are valid only to the extent that the minimum-current assumption is valid. (Some authors have speculated that a self-limited MITL operates not at the minimum anode current, but instead at the current that is obtained in a minimum-energy calculation [12,20]. We discuss such a calculation in Appendix A.)

For all of the self-limited experiments summarized in Table II, we list measured values of V_a and Z_0 in the first column, and measured values of $I_{a,\min}$, $I_{f,\min}$, and $Z_{f,\min}$ in the second. To compare the self-limited measurements with theory, we make the arbitrary and simplifying assumption that the measured values of V_a and Z_0 are given quantities, and use these to *predict* values of $I_{a,\min}$, $I_{f,\min}$, and $Z_{f,\min}$, as determined by the collisional and collisionless models.

One set of measurements listed in Table II was performed on a MITL that was not self-limited. In such a case, the total anode current I_a is determined, in part, by the load. To compare these measurements with theory, we make the arbitrary and simplifying assumption that the measured values of V_a, Z_0, and I_a are given quantities, and use these to predict values of I_f and Z_f.

Most of the measurements summarized in the table were performed on MITLs with coaxial cylindrical electrodes (with the inner conductor at a negative potential); one set of measurements was obtained in an approximately planar geometry. For the coaxial-geometry experiments, the predictions of Eq. (B1) are given in the third column of Table II; for the single experiment conducted in planar geometry, the collisional predictions of Eq. (58) are given. The collisionless predictions given in the fourth column are those of the parapotential (Creedon) model [Eq. (75)], which appears to be the collisionless model most often quoted in the literature [42,44]. Equation (75) is valid for planar electrodes, as well as for coaxial electrodes when the inner electrode is at a negative potential with respect to the outer.

The data presented in Table II that were obtained by Bernstein and Smith [6] were taken on a 4.6-m-long coax-

TABLE II. Comparison of measurements with theoretical predictions. The steady-state collisional-MITL model [Eqs. (58) and (B1)] is valid only when the drift of electrons toward the anode has had sufficient time to broaden the electron sheath until a steady-state configuration has been achieved. The parapotential collisionless model [Eq. (75)], developed by Creedon [8,9], is valid in the opposite limit; i.e., when collisional broadening of the sheath can be neglected. We expect experimentally observed MITL parameters to fall between the values predicted in these two limits. For the planar-MITL experiment listed in the first column, we present in the third column the predictions of Eq. (58). For the coaxial-MITL experiments, we present the predictions of Eq. (B1). We note that all the discrepancies in this table between the measurements and *collisionless* predictions can be accounted for by experimental uncertainties. However, all the discrepancies are in a direction that would be consistent with the existence of collisions.

Reference	Measurements	Predictions of the collisional model [Eq. (58) or (B1)]	Predictions of the parapotential collisionless model [Eq. (75)]
Bernstein and Smith [6] ($V_a = 14$ MV, $Z_0 = 47\ \Omega$, coaxial, self-limited)	$I_{a,\min} = 400$ kA	$I_{a,\min} = 590$ kA	$I_{a,\min} = 350$ kA
Bergeron, Poukey, Di Capua, and Pellinen [13] ($V_a = 1.5$ MV, $Z_0 = 41.6\ \Omega$, coaxial, self-limited)	$I_{a,\min} = 64$ kA $I_{f,\min} = 37$ kA $Z_{f,\min} = 26\ \Omega$	$I_{a,\min} = 70$ kA $I_{f,\min} = 48$ kA $Z_{f,\min} = 23\ \Omega$	$I_{a,\min} = 57$ kA $I_{f,\min} = 22$ kA $Z_{f,\min} = 33\ \Omega$
Shope and colleagues [15] ($V_a = 1.3$ MV, $Z_0 = 11\ \Omega$, coaxial, self-limited)	$I_{a,\min}Z_0/V_a \sim 1.9$	$I_{a,\min}Z_0/V_a = 1.82$	$I_{a,\min}Z_0/V_a = 1.64$
Shope and colleagues [15] ($V_a = 3.5$–10 MV, $Z_0 = 139\ \Omega$, coaxial, self-limited)	$I_{a,\min}Z_0/V_a \sim 1.56$	$I_{a,\min}Z_0/V_a = 2.46$	$I_{a,\min}Z_0/V_a = 1.37$–1.21
Di Capua and Pellinen [17] ($V_a = 1.8$ MV, $Z_0 = 41.6\ \Omega$, coaxial, self-limited)	$I_{a,\min} = 71$ kA $I_{f,\min} = 41$ kA $Z_{f,\min} = 28\ \Omega$	$I_{a,\min} = 84$ kA $I_{f,\min} = 57$ kA $Z_{f,\min} = 23\ \Omega$	$I_{a,\min} = 66$ kA $I_{f,\min} = 27$ kA $Z_{f,\min} = 34\ \Omega$
Sanford and colleagues [40] ($V_a = 0.85$ MV, $Z_0 = 28.3\ \Omega$, $I_a = 84$ kA, planar, *not* self-limited)	$I_f = 11$ kA $Z_f = 20\ \Omega$	$I_f = 14$ kA $Z_f = 19\ \Omega$	$I_f = 6$ kA $Z_f = 27\ \Omega$
Sanford and colleagues [42,44] ($V_a = 18.4$ MV, $Z_0 = 34\ \Omega$, coaxial, self-limited)	$I_{a,\min} = 655$ kA $I_{f,\min} = 470$ kA $Z_{f,\min} = 29\ \Omega$	$I_{a,\min} = 1038$ kA $I_{f,\min} = 710$ kA $Z_{f,\min} = 19\ \Omega$	$I_{a,\min} = 621$ kA $I_{f,\min} = 406$ kA $Z_{f,\min} = 32\ \Omega$

ial MITL with $Z_0 = 47\ \Omega$ and a 34-cm AK gap. At 14 MV, the MITL's self-limited anode current $I_{a,\min} = 400$ kA (i.e., the self-limited impedance $V_a/I_{a,\min} = 35\ \Omega$). As indicated by Table II, the measured value of $I_{a,\min}$ falls between the collisional and collisionless predictions.

The measurements by Bergeron, Poukey, Di Capua, and Pellinen [13] listed in Table II were performed on a 10-m-long coaxial MITL with $Z_0 = 41.6\ \Omega$ and a 2.86-cm AK gap. These authors find that at an axial distance of 7.5 m from the point at which the power pulse is launched into the MITL, the measured values of V_a, $I_{a,\min}$, $I_{f,\min}$, and $Z_{f,\min}$ are approximately 1.5 MV, 64 kA, 37 kA, and 26 Ω, respectively [13]. Assuming that the measured values of V_a and Z_0 are correct, we compare in Table II the measurements of $I_{a,\min}$, $I_{f,\min}$, and $Z_{f,\min}$ with the predictions of the collisional and collisionless models.

Shope and colleagues [15] describe measurements performed on a 0.5-m-long coaxial MITL with $Z_0 = 11\ \Omega$ and a 1.3-cm AK gap. When V_a is 1.3 MV, the measured value of $I_{a,\min}Z_0/V_a$ is $\sim$1.9. [Please see Fig. 4(a) of [15]. This figure actually plots the ratio $V_a/I_{a,\min}Z_0$ as a function of V_a.] The measured value of

$I_{a,\min}Z_0/V_a$ is somewhat higher than the prediction of the collisional model.

Shope and colleagues also describe measurements performed on a 1.37-m-long coaxial MITL with $Z_0 = 139\ \Omega$ and a 68.5-cm AK gap [15]. When V_a is varied between 3.5 and 10 MV, the measured values of $I_{a,\min}Z_0/V_a$ remain roughly constant at ~1.56. [Please see Fig. 4(b) of [15]. This figure actually plots the ratio $V_a/I_{a,\min}Z_0$ as a function of V_a.] As indicated in Table II, the measurements fall between the predictions of the collisional and collisionless models.

The measurements by Di Capua and Pellinen [17] were performed on a 10-m-long coaxial MITL with $Z_0 = 41.6\ \Omega$ and a 2.86-cm AK gap, which is the same MITL described in [13]. At an axial distance of 7.5 m from the point at which the power pulse is launched into the MITL, the estimated value of V_a is 1.8 MV, and the measured values of $I_{a,\min}$ and $I_{k,\min}$ are 71 and 30 kA, respectively. (Please see Fig. 6 of [17].) Hence $I_{f,\min}$ and $Z_{f,\min}$ are approximately 41 kA and 28 Ω. Assuming that the measured values of V_a and Z_0 are correct, the measured values of $I_{a,\min}$, $I_{f,\min}$ and $Z_{f,\min}$ fall between the predictions of the collisional and collisionless models.

In Ref. [40], Sanford and co-workers report measurements performed on an approximately planar MITL with $Z_0 = 28.3\ \Omega$ and an AK gap of ~2.2 cm. At peak voltage ($V_a = 0.85$ MV) this MITL is not self-limited (because of the load), and the measured values of I_a, I_f, and Z_f are 84 kA, 11 kA, and 20 Ω, respectively. Assuming that the measured values of V_a, Z_0, and I_a are given quantities, we compare in Table II the measured values of I_f and Z_f to the collisional and collisionless predictions.

References [42,44] describe experiments performed by Sanford and colleagues on the HERMES-III accelerator. The coaxial HERMES-III MITL has a vacuum impedance of $Z_0 = 34\ \Omega$ and a 14.1-cm AK gap. When the measured MITL voltage V_a is 18.4 MV and the MITL is self-limited, the measured values of $I_{a,\min}$, $I_{f,\min}$ and $Z_{f,\min}$ are 655 kA, 470 kA, and 29 Ω, respectively [42,44]. (Reference [42] presents a detailed discussion of the HERMES-III voltage measurements. This article concludes that the peak voltage for the experiments in question is 18.7 MV, which is an average of the 5 measurements listed in Table I of Ref. [42]. Since one of the 5 measurements uses the collisionless parapotential MITL model, we exclude this measurement, and obtain from the remaining 4 measurements a value of 18.4 MV.) Assuming that the measured values of V_a and Z_0 are correct, we find that the measured values of $I_{a,\min}$, $I_{f,\min}$ and $Z_{f,\min}$ fall between the values predicted by the collisional and collisionless models, as indicated in Table II.

Other evidence of collisional broadening of the electron sheath exists in the HERMES-III data, as indicated by Fig. 8 of Ref. [44]. This figure suggests that measured spatial distributions of the flow electrons are significantly broader than predicted by particle-in-cell simulations. In addition, Ref. [44] observes that 2D particle-in-cell simulations of the experiments show evidence of electromagnetic-field fluctuations, which increase the energy of some of the electrons to 24 MV, significantly above the nominal MITL voltage.

We note that the experimental results and theoretical predictions listed in Table II have *not* been corrected for the decrease in the MITL AK gap due to the expansion of the cathode plasma. Assuming this plasma expands at 2 cm/μs, and that it is a perfect conductor, we find that the plasma does not significantly affect the results presented in Table II, due to the large gaps and short pulse lengths of the experiments. The most significant correction would be to the 1.3-MV measurements reported by Shope and colleagues [15], since these were performed with a 1.3-cm AK gap. Assuming that the cathode plasma had expanded for 40 ns by the time these measurements were made, the MITL impedance Z_0 would have been reduced from 10.94 to 10.21 Ω, which would have reduced the measured value of $I_{a,\min}Z_0/V_a$ from 1.9 to 1.77. The corresponding collisional-model prediction for this experiment would change by less than 1%, since the theoretical value of $I_{a,\min}Z_0/V_a$ is an insensitive function of Z_0. The corresponding collisionless-model prediction for the ratio $I_{a,\min}Z_0/V_a$ is independent of Z_0.

We caution that the discrepancies summarized in Table II between the measurements and *collisionless*-model predictions can be accounted for by the usual experimental uncertainties involved in measuring MITL voltages and currents. However, all the discrepancies appear to be in a direction that would be consistent with the existence of collisions.

We also caution that the measurements listed in Table II can be meaningfully compared to the theoretical predictions only if most of the flow electrons in the experiments were emitted from the MITL cathode, and not from other vacuum-section components, such as the insulator surfaces of the MITL's vacuum interface.

VIII. DISCUSSION

The principal prediction of this article is that the measured electrical parameters of a MITL will fall *between* the values predicted by the idealized collisional and collisionless models. We also predict that, when all other quantities are held constant, collisional effects will increase as the length of a MITL is increased (i.e., as the electrons are given more time to drift across the AK gap), or as the AK gap is decreased (as the time required to drift across the gap is decreased).

As discussed in Secs. II B 2 and VII, several measurements *suggest* that collisional effects can, in fact, have non-negligible effects on the electrical performance of physically relevant MITLs. Hence collisions may have to be considered in the design of pulsed-power accelerators that

use MITLs to deliver electromagnetic power and energy to a load.

We note that collisions may be relatively less troublesome for applications in which the MITL delivers power and energy to an electron-beam-diode load. In this case, even if the flow electrons drift across most of the MITL gap by the time the power pulse arrives at the diode, the flow electrons may simply join the electrons generated at the diode, without adversely affecting the electrical performance of the MITL-diode system. However, even in this case collisional effects would alter the electrical characteristics of the MITL.

When a MITL delivers power to other types of loads, such as a z pinch [45–47], then when collisions significantly increase the current flowing in the electron sheath, less *bound* current is carried by the MITL's cathode. In this case, less bound current (i.e., less than predicted by the collisionless models) is available to drive the load.

For either type of application, the collisional model developed in Sec. III, Sec. IV, and Appendix B provides upper bounds on the effects collisions can have on the electrical performance of a MITL.

ACKNOWLEDGMENTS

The authors would very much like to thank J. Boyes, R. Clark, D. Fehl, T. Hughes, M. Johnson, M. Kiefer, R. Leeper, M. K. Matzen, D. McDaniel, B. Oliver, B. Peyton, J. Porter, J. Puissant, P. Reynolds, S. Rosenthal, K. Struve, A. Tagliaferro, D. Van De Valde, E. Weinbrecht, and D. Welch for critical contributions, and T. Culter, S. Rosenthal, M. Savage, and S. Slutz for graciously reviewing this article. We also wish to acknowledge our many other colleagues at Sandia National Laboratories, C-Lec Plastics, EG&G, Ktech Corporation, Mission Research Corporation, Prodyn Tecnologies, Team Specialty Products, Titan–Pulse Sciences Division, Voss Scientific, and Votaw for their sustained support of this work. Sandia is a multiprogram laboratory operated by Sandia Corporation, a Lockheed Martin Company, for the United States Department of Energy's National Nuclear Security Administration under Contract No. DE-AC04-94AL85000.

APPENDIX A: MINIMUM-ENERGY OPERATING POINT

As discussed in Secs. I, IV A, and VI A, we assume in this article that, when a MITL is self-limited, the MITL anode current $I_a = I_{a,\min}$, where $I_{a,\min}$ is the minimum required to establish magnetic insulation.

Several workers have *speculated* that a self-limited MITL may operate not at $I_{a,\min}$, but instead at the anode current that is obtained when a nominal value of the total MITL energy per unit length W is minimized [12,20]. This energy is assumed to be the sum of the following components: the energy of the steady-state electric field, the steady-state magnetic field, and the laminar component of the flow-electron velocities. This sum can be expressed as follows [12,20,31]:

$$W = w \int_0^g \left(\frac{B_z^2}{2\mu_0} + \frac{\varepsilon_0 E_x^2}{2} + nmc^2(\gamma - 1) \right) dx. \qquad \text{(A1)}$$

The quantities V_a, w, and g are *held constant* while χ [Eq. (60)] is varied to determine the anode current at which W reaches its minimum value.

We have calculated the minimum-energy operating point of a collisional MITL using the method described above, and find that the anode current and flow impedance at minimum total energy are, to first order, the same as the values obtained at minimum anode current. This agreement, which is similar to the agreement demonstrated in Refs. [12,20,31] for collisionless MITL models, is explained by Slutz in Ref. [31].

However, it is not clear that the correct energy to minimize is the *total* energy, as defined above, instead of a suitably defined *potential* energy, as is normally done for a stability analysis [50,54]. It is also not clear whether the minimum-energy calculation described above is consistent with other stability analyses that have been performed for MITL-flow electrons [16,21,24,28,29,33,49,51,52,55,56,63,64]. In addition, it is not clear what dissipative mechanism is involved when a MITL relaxes from a higher total-energy state to a lower one. Furthermore, the minimum-energy calculation described above neglects any change in the nonlaminar component of the flow-electron velocities as a MITL relaxes to a lower-energy state. The calculation also neglects any change in the energy of fluctuating electrostatic and electromagnetic fields. It is also not clear that the voltage of a propagating power pulse in a self-limited MITL stays constant as the pulse relaxes to a lower-energy state, while the pulse propagates along the line. In fact, for the experiments described in Ref. [11], the MITL voltage is observed to decrease linearly with the distance that the pulse has propagated, as indicated by Fig. 2 of [11].

A rigorous proof that a self-limited MITL operates at *minimum total energy* has not yet been presented in the literature. (In Ref. [20], Wang and Di Capua mention that such a proof was being derived, but apparently it has not yet been published.) It is important to note that a proof that a self-limited MITL operates at *minimum anode current* has also has not yet been published. The only motivations for the use of either assumption appear to be that they are in approximate agreement with other, and with experiment. In other words, there presently appears to be no *theoretical* justification for either assumption.

A resolution of this issue is outside the scope of the present article. Instead, we simply follow previous work [42,44], and assume in this article that when a MITL is self-limited, the MITL anode current is, at given values of

V_a and Z_0, the minimum required to establish magnetic insulation.

APPENDIX B: COLLISIONAL MITL WITH COAXIAL ELECTRODES

The collisional-MITL model developed in Secs. III and IV assumes that the MITL has planar electrodes in a parallel-plate geometry. The model also assumes that the MITL is 1D; i.e., that the AK gap is small compared to the width of the electrodes. Under these assumptions, the general relation between V_a, I_a, I_k, and Z_0 is given by Eq. (58).

When we assume that the MITL consists of coaxial cylindrical electrodes, and that the inner electrode is at a negative potential with respect to the outer, we obtain instead of Eq. (58) the following relation:

$$V_a = \frac{c\mu_0 r_k}{\pi g} I_a \frac{(\chi-1)^{1/2}}{\chi}(h_1 + h_2 + h_3). \tag{B1}$$

The quantity r_k is the radius of the inner (cathode) conductor; the terms h_1, h_2, and h_3 are defined as follows:

$$h_1 \equiv \frac{(g/r_k) - \chi + 1}{(\chi-1)^{1/2}} \sinh^{-1}\left(\frac{\chi-1}{2}\right)^{1/2}, \tag{B2}$$

$$h_2 \equiv -\left[\frac{2g}{r_k} - \chi + 1\right]^{1/2} \tan^{-1}\left(\frac{(2g/r_k) - \chi + 1}{\chi+1}\right)^{1/2}, \tag{B3}$$

$$h_3 \equiv \frac{g(\chi+1)^{1/2}}{2r_k}. \tag{B4}$$

The geometric impedance of the MITL is given by

$$Z_0 = \left(\frac{\mu_0}{4\pi^2\varepsilon_0}\right)^{1/2} \ln\left(\frac{r_k + g}{r_k}\right). \tag{B5}$$

Equations (B1)–(B5) give the general relation between V_a, I_a, I_k, and Z_0 for a steady-state collisional MITL with coaxial electrodes, assuming that the inner conductor is at a negative potential with respect to the outer. Equations (B1)–(B4) are given *explicitly* in terms of V_a, I_a, and I_k; these equations are given *implicitly* in terms of Z_0, since these equations are more naturally expressed in terms of g and r_k.

Equation (B3) is, of course, applicable only when

$$\left[\frac{2g}{r_k} - \chi + 1\right] \geq 0. \tag{B6}$$

When instead

$$\left[\frac{2g}{r_k} - \chi + 1\right] \leq 0, \tag{B7}$$

then

$$h_2 \equiv \left[\chi - 1 - \frac{2g}{r_k}\right]^{1/2} \tanh^{-1}\left(\frac{\chi - 1 - (2g/r_k)}{\chi+1}\right)^{1/2}. \tag{B8}$$

In planar geometry, since $h(\chi)$ [Eq. (59)] is independent of V_a and Z_0, the constants on the right-hand sides of Eqs. (64)–(67), (70), and (71) are also independent of V_a and Z_0. In coaxial geometry, the sum $h_1 + h_2 + h_3$ of Eq. (B1) is independent of V_a, but not Z_0. Hence the constants on the right-hand sides of Eqs. (64)–(67), (70), and (71) are, for the coaxial case, functions of Z_0.

When $Z_0 = 40\ \Omega$, and when a MITL is *minimally insulated* ($I_a = I_{a,\min}$), we obtain instead of Eqs. (64)–(67) the following relations:

$$I_{a,\min} = 1.94\frac{V_a}{Z_0}, \tag{B9}$$

$$\chi_{\min} \equiv \left.\frac{I_a}{I_k}\right|_{\min} = 3.13, \tag{B10}$$

$$I_{f,\min} = 0.681 I_{a,\min} = 1.32\frac{V_a}{Z_0}, \tag{B11}$$

$$Z_{f,\min} = 0.543 Z_0. \tag{B12}$$

The constants on the right-hand sides of Eqs. (B9)–(B12) are within 9% of the constants of Eqs. (64)–(67). The differences between the planer and coaxial relations decrease as Z_0 is decreased from $40\ \Omega$; the differences become negligible as $Z_0 \to 0$.

When $Z_0 = 40\ \Omega$, and when a MITL is *well insulated* ($I_a \gg I_{a,\min}$), we obtain instead of Eqs. (70) and (71) the following relations:

$$I_f = \frac{1.30 V_a^2}{I_a Z_0^2}, \tag{B13}$$

$$Z_f = 0.621 Z_0. \tag{B14}$$

The constant on the right-hand side of Eq. (B13) is within 16% of the constant of Eq. (70); the constants of Eqs. (B14) and (71) are within 7%. As before, the differences between the planar and coaxial relations become negligible as $Z_0 \to 0$.

APPENDIX C: FORCE-BALANCE EQUATION FOR A STEADY-STATE 3D MITL

According to Stratton [80], the total electric force on an arbitrary steady-state 3D *charge* distribution inside a volume Ω, that is enclosed by the surface Σ, is given by

$$-\int_\Omega en\mathbf{E}d\upsilon = \varepsilon_0 \int_\Sigma \left[(\mathbf{E}\cdot\mathbf{n})\mathbf{E} - \frac{E^2}{2}\mathbf{n}\right] da. \tag{C1}$$

In this expression $d\upsilon$ is the differential volume element, $\mathbf{n}$

is the unit vector normal to the surface Σ at differential surface element da, and E is the magnitude of $\mathbf{E}$.

The total magnetic force on an arbitrary steady-state 3D *current* distribution in a volume Ω enclosed by surface Σ is given by [80]

$$\int_\Omega \mathbf{j} \times \mathbf{B} dv = \frac{1}{\mu_0} \int_\Sigma \left[(\mathbf{B} \cdot \mathbf{n})\mathbf{B} - \frac{B^2}{2}\mathbf{n} \right] da, \qquad \text{(C2)}$$

where $\mathbf{j}$ is the current density and B is the magnitude of $\mathbf{B}$.

Assuming that the only significant forces on the flow-electron sheath in a 3D MITL are the electric and magnetic forces given by Eqs. (C1) and (C2), respectively, then a *necessary* condition for a 3D MITL to be in a steady state is that the total Lorentz force on the MITL's electron sheath equals zero. This condition can be expressed as

$$\int_\Sigma \left[(\mathbf{E} \cdot \mathbf{n})\mathbf{E} - \frac{E^2}{2}\mathbf{n} \right] da = c^2 \int_\Sigma \left[\frac{B^2}{2}\mathbf{n} - (\mathbf{B} \cdot \mathbf{n})\mathbf{B} \right] da. \qquad \text{(C3)}$$

Equation (C3) is valid only when other forces on the flow electrons [such as those due to collisions, the $\nabla(\boldsymbol{\mu} \cdot \mathbf{B})$ force due to the intrinsic magnetic moment $\boldsymbol{\mu}$ of the electron [77], and radiation damping [77]] can be neglected.

For the steady-state 1D planar MITL illustrated in Fig. 1, Eq. (C3) reduces directly to Eq. (50) when $E_k \equiv E_x(0) = 0$. Hence Eq. (50) is approximately valid for any steady-state 1D planar MITL when $E_k \equiv E_x(0) = 0$, and all forces on the electrons other than the Lorentz force can be neglected.

[1] R. K. Parker, R. E. Anderson, and C. V. Duncan, J. Appl. Phys. **45**, 2463 (1974).
[2] G. A. Mesyats and D. I. Proskurovsky, *Pulsed Electrical Discharge in Vacuum* (Springer-Verlag, Berlin, 1989).
[3] *High Voltage Vacuum Insulation*, edited by R. Latham (Academic, London, 1995).
[4] T. H. Martin, IEEE Trans. Nucl. Sci. **16**, No. 3, 59 (1969).
[5] F. Winterberg, in *Physics of High Energy Density* (Academic, New York, 1971), p. 393.
[6] B. Bernstein and I. Smith, IEEE Trans. Nucl. Sci. **20**, No. 3, 294 (1973).
[7] A. Ron, A. A. Mondelli, and N. Rostoker, IEEE Trans. Plasma Sci. **1**, 85 (1973).
[8] J. M. Creedon, J. Appl. Phys. **46**, 2946 (1975).
[9] J. M. Creedon, J. Appl. Phys. **48**, 1070 (1977).
[10] K. D. Bergeron, Phys. Fluids **20**, 688 (1977).
[11] D. H. McDaniel, J. W. Poukey, K. D. Bergeron, J. P. VanDevender, and D. L. Johnson, in *Proceedings of the 2nd International Topical Conference on High-Power Electron and Ion-Beam Research and Technology*, edited by J. A. Nation and R. N. Sudan (Cornell University, Ithaca, New York, 1977), p. 819.
[12] E. I. Baranchikov, A. V. Gordeev, V. D. Korolev, and V. P. Smirnov, Sov. Phys. Tech. Phys. **48**, 1058 (1978).
[13] K. D. Bergeron, J. W. Poukey, M. S. Di Capua, and D. G. Pellinen, in *Proceedings of the VII International Symposium on Discharges and Electrical Insulation in Vacuum*, edited by G. W. Kuswa, R. Bartsch, A. H. Guenther, J. A. Panitz, and M. Kristiansen (Sandia National Laboratories, Albuquerque, NM, 1978), p. E2-1.
[14] J. W. Poukey and K. D. Bergeron, Appl. Phys. Lett. **32**, 8 (1978).
[15] S. Shope, J. W. Poukey, K. D. Bergeron, D. H. McDaniel, A. J. Toepfer, and J. P. VanDevender, J. Appl. Phys. **49**, 3675 (1978).
[16] K. D. Bergeron and J. W. Poukey, J. Appl. Phys. **50**, 4996 (1979).
[17] M. S. Di Capua and D. G. Pellinen, J. Appl. Phys. **50**, 3713 (1979).
[18] M. S. Di Capua and T. S. Sullivan, in *Proceedings of the 2nd IEEE International Pulsed Power Conference*, edited by A. H. Guenther and M. Kristiansen (IEEE, Piscataway, NJ, 1979), p. 483.
[19] J. P. VanDevender, J. Appl. Phys. **50**, 3928 (1979).
[20] M. Y. Wang and M. S. Di Capua, J. Appl. Phys. **51**, 5610 (1980).
[21] J. Swegle and E. Ott, Phys. Rev. Lett. **46**, 929 (1981).
[22] J. Swegle and E. Ott, Phys. Fluids **24**, 1821 (1981).
[23] J. P. VanDevender, J. T. Crow, B. G. Epstein, D. H. McDaniel, C. W. Mendel, Jr., E. L. Neau, J. W. Poukey, J. P. Quintenz, D. B. Seidel, and R. W. Stinnett, Physica (Amsterdam) **104C**, 104 (1981).
[24] J. Swegle, Phys. Fluids **25**, 1282 (1982).
[25] V. L. Bailey, J. M. Creedon, B. M. Ecker, and H. I. Helava, J. Appl. Phys. **54**, 1656 (1983).
[26] M. S. Di Capua, IEEE Trans. Plasma Sci. **11**, No. 3, 205 (1983).
[27] C. W. Mendel, Jr., D. B. Seidel, and S. E. Rosenthal, Laser Part. Beams **1**, 311 (1983).
[28] J. Swegle, Phys. Fluids **26**, 1670 (1983).
[29] C. W. Mendel, Jr., J. A. Swegle, and D. B. Seidel, Phys. Rev. A **32**, 1091 (1985).
[30] P. A. Miller and C. W. Mendel, Jr., J. Appl. Phys. **61**, 529 (1987).
[31] S. A. Slutz, J. Appl. Phys. **61**, 2087 (1987).
[32] R. I. Lawconnell and J. Neri, Phys. Fluids B **2**, 629 (1990).
[33] N. A. Krall and S. E. Rosenthal, J. Appl. Phys. **70**, 2542 (1991).
[34] C. W. Mendel, Jr., S. E. Rosenthal, and D. B. Seidel, Phys. Rev. A **45**, 5854 (1992).
[35] C. W. Mendel, Jr., M. E. Savage, D. M. Zagar, W. W. Simpson, T. W. Grasser, and J. P. Quintenz, J. Appl. Phys. **71**, 3731 (1992).
[36] C. W. Mendel, Jr. and S. E. Rosenthal, Phys. Plasmas **2**, 1332 (1995).
[37] C. W. Mendel, Jr. and S. E. Rosenthal, Phys. Plasmas **3**, 4207 (1996).
[38] C. W. Mendel, Jr. and D. B. Seidel, Phys. Plasmas **6**, 4791 (1999).
[39] B. V. Oliver, T. C. Genoni, T. P. Hughes, and D. R. Welch (to be published).
[40] T. W. L. Sanford, J. R. Lee, J. A. Halbleib, J. P. Quintenz, R. S. Coats, W. A. Stygar, R. E. Clark, D. L. Faucett, D. Webb, C. E. Heath, P. W. Spence, J. Kishi, L. G. Schlitt, and D. Morton, J. Appl. Phys. **59**, 3868 (1986).

[41] S. E. Rosenthal, IEEE Trans. Plasma Sci. **19**, 822 (1991).
[42] T. W. L. Sanford, J. A. Halbleib, L. J. Lorence, Jr., J. G. Kelly, P. J. Griffin, J. W. Poukey, R. C. Mock, W. H. McAtee, and K. A. Mikkelson, Rev. Sci. Instrum. **63**, 4795 (1992).
[43] M. E. Cuneo, J. W. Poukey, C. W. Mendel, Jr., S. E. Rosenthal, D. L. Hanson, D. L. Smith, J. E. Maenchen, D. F. Wenger, and M. A. Bernard, *Proceedings of the 9th IEEE International Pulsed Power Conference, Albuquerque, NM, 1993*, edited by K. R. Prestwich and W. L. Baker (IEEE, Piscataway, NJ, 1993), p. 423.
[44] T. W. L. Sanford, J. W. Poukey, J. A. Halbleib, R. C. Mock, and W. H. McAtee, J. Appl. Phys. **73**, 2004 (1993).
[45] W. A. Stygar, R. B. Spielman, G. O. Allshouse, C. Deeney, D. R. Humphreys, H. C. Ives, F. W. Long, T. H. Martin, M. K. Matzen, D. H. McDaniel, C. W. Mendel, Jr., L. P. Mix, T. J. Nash, J. W. Poukey, J. J. Ramirez, T. W. L. Sanford, J. F. Seamen, D. B. Seidel, J. W. Smith, D. M. Van De Valde, R. W. Wavrik, P. A. Corcoran, J. W. Douglas, I. D. Smith, M. A. Mostrom, K. W. Struve, T. P. Hughes, R. E. Clark, R. W. Shoup, T. C. Wagoner, T. L. Gilliland, and B. Peyton, in *Proceedings of the 11th IEEE International Pulsed Power Conference, Baltimore, MD, 1997*, edited by G. Cooperstein and I. Vitkovitsky (IEEE, Piscataway, NJ, 1997), p. 591.
[46] H. C. Ives, D. M. Van De Valde, F. W. Long, J. W. Smith, R. B. Spielman, W. A. Stygar, R. W. Wavrick, and R. W. Shoup, in *Proceedings of the 11 th IEEE International Pulsed Power Conference, Baltimore, MD, 1997*, (Ref. [45]), p. 1602.
[47] P. A. Corcoran, J. W. Douglas, I. D. Smith, P. W. Spence, W. A. Stygar, K. W. Struve, T. H. Martin, R. B. Spielman, and H. C. Ives, in *Proceedings of the 11th IEEE International Pulsed Power Conference* (Ref. [45]), p. 466.
[48] I. Langmuir, Phys. Rev. **26**, 585 (1925).
[49] O. Buneman, in *Cross Field Microwave Devices*, edited by F. Okress (Academic Press, New York, 1961), Vol. 1, p. 209.
[50] L. Spitzer, *Physics of Fully Ionized Gases* (Wiley, New York, 1962).
[51] O. Bunemen, R. H. Levy, and L. M. Linson, J. Appl. Phys. **37**, 3203 (1966).
[52] K. Mouthaan and C. Süsskind, J. Appl. Phys. **37**, 2598 (1966).
[53] S. Ichimaru, *Basic Principles of Plasma Physics* (W.A. Benjamin, Reading, Massachusetts, 1973).
[54] N. A. Krall and A. W. Trivelpiece, *Principles of Plasma Physics* (McGraw-Hill, New York, 1973).
[55] R. V. Lovelace and E. Ott, Phys. Fluids **17**, 1263 (1974).
[56] E. Ott and R. V. Lovelace, Appl. Phys. Lett. **27**, 378 (1975).
[57] F. F. Chen, *Introduction to Plasma Physics* (Plenum, New York, 1976).
[58] T. J. Orzechowski and G. Bekefi, Phys. Fluids **19**, 43 (1976).
[59] G. Bekefi and T. J. Orzechowski, in *Proceedings of the IEEE International Pulsed Power Conference*, edited by Texas Tech University and IEEE (IEEE, Piscataway, NJ, 1976), p. IIC6-1.
[60] R. C. Davidson and N. A. Krall, Nucl. Fusion **17**, 1313 (1977).
[61] T. J. Orzechowski and G. Bekefi, Phys. Fluids **22**, 978 (1979).
[62] R. N. Sudan, in *Proceedings of the 4th International Topical Conference on High-Power Electron and Ion-Beam Research and Technology*, edited by H. J. Doucet and J. M. Buzzi (Ecole Polytechnique, Palaiseau, France, 1981), p. 389.
[63] R. C. Davidson, K. T. Tsang, and J. A. Swegle, Phys. Fluids **27**, 2332 (1984).
[64] R. Davidson and K. T. Tsang, Phys. Rev. A **30**, 488 (1984).
[65] Y. Maron, Phys. Fluids **27**, 285 (1984).
[66] M. P. Desjarlais, Phys. Rev. Lett. **59**, 2295 (1987).
[67] M. P. Desjarlais, Phys. Fluids B **1**, 1709 (1989).
[68] H. R. Kaufman, J. Vac. Sci. Technol. B **8**, 107 (1990).
[69] T. Westermann and R. Schuldt, Phys. Fluids B **5**, 4408 (1993).
[70] T. D. Pointon, M. P. Desjarlais, D. B. Seidel, S. A. Slutz, R. S. Coats, M. L. Kiefer, and J. P. Quintenz, Phys. Plasmas **1**, 429 (1994).
[71] G. Lister, J. Vac. Sci. Technol. A **14**, 2736 (1996).
[72] W. A. Stygar, G. A. Gerdin, and D. L. Fehl, Phys. Rev. E **66**, 046417 (2002).
[73] E. Buckingham, Phys. Rev. **4**, 345 (1914).
[74] W. J. Duncan, *Physical Similarity and Dimensional Analysis* (Edward Arnold & Co., London, 1953).
[75] G. I. Barenblatt, *Scaling* (Cambridge University Press, Cambridge, England, 2003).
[76] M. S. Longair, *Theoretical Concepts in Physics* (Cambridge University Press, Cambridge, England, 2003).
[77] J. D. Jackson, *Classical Electrodynamics* (Wiley, New York, 1975).
[78] R. P. Feynman, R. B. Leighton, and M. Sands, *The Feynman Lectures on Physics* (Addison-Wesley, Reading, MA, 1963), p. 43–49.
[79] H. B. Dwight, *Tables of Integrals and Other Mathematical Data* (MacMillan, New York, 1961), p. 76.
[80] J. A. Stratton, *Electromagnetic Theory* (McGraw-Hill, New York, 1941), Sec. 2.